EUROPEAN ORGANISATION FOR NUCLEAR RESEARCH (CERN)

Submitted to: Physics Letters B

CERN-EP-2023-029
20th March 2023

Comparison of inclusive and photon-tagged jet suppression in 5.02 TeV Pb+Pb collisions with ATLAS

The ATLAS Collaboration

Parton energy loss in the quark–gluon plasma (QGP) is studied with a measurement of photon-tagged jet production in 1.7 nb^{-1} of Pb+Pb data and 260 pb^{-1} of pp data, both at $\sqrt{s_{\text{NN}}}$ = 5.02 TeV, with the ATLAS detector. The process $pp \to \gamma$+jet+X and its analogue in Pb+Pb collisions is measured in events containing an isolated photon with transverse momentum (p_{T}) above 50 GeV and reported as a function of jet p_{T}. This selection results in a sample of jets with a steeply falling p_{T} distribution that are mostly initiated by the showering of quarks. The pp and Pb+Pb measurements are used to report the nuclear modification factor, R_{AA}, and the fractional energy loss, S_{loss}, for photon-tagged jets. In addition, the results are compared with the analogous ones for inclusive jets, which have a significantly smaller quark-initiated fraction. The R_{AA} and S_{loss} values are found to be significantly different between those for photon-tagged jets and inclusive jets, demonstrating that energy loss in the QGP is sensitive to the colour-charge of the initiating parton. The results are also compared with a variety of theoretical models of colour-charge-dependent energy loss.

Contents

1 Introduction

Ultra-relativistic collisions of heavy nuclei at the Large Hadron Collider (LHC) and the Relativistic Heavy Ion Collider (RHIC) produce a hot, deconfined nuclear medium known as the quark–gluon plasma (QGP). The QGP exhibits interesting emergent phenomena, such as a collective evolution that suggests it is a strongly coupled fluid well described by hydrodynamics [1–3]. The dense colour field arising from the deconfined colour charges that makes up the QGP is opaque to high-energy quarks and gluons attempting to pass through it. This results in hard-scattered partons suffering energy loss and a modification of their showering processes as they traverse the QGP. This phenomenon is known as *jet quenching*, and results in a wide variety of experimental signatures – see Ref. [4] for a recent review.

A straightforward and broadly used signature of jet quenching is the suppression of jet production at fixed transverse momentum[1] (p_{T}) in Pb+Pb collisions compared to pp collisions. This is quantified by the nuclear modification factor, R_{AA}, which is defined as the ratio of the observed yield in Pb+Pb collisions to the expectation from an equivalent number of nucleon–nucleon (NN) collisions, i.e., without jet quenching effects from the formation of a QGP. This expectation is calculated as the cross-section in pp collisions, scaled by the mean value of the nuclear thickness function in the corresponding Pb+Pb collisions, $\langle T_{\mathrm{AA}} \rangle$ [5]. The R_{AA} is therefore defined as

$$R_{\mathrm{AA}} = \frac{1}{N_{\mathrm{evt}}} \frac{\mathrm{d}^2 N^{\mathrm{Pb+Pb}}}{\mathrm{d}p_{\mathrm{T}}\mathrm{d}\eta} \Big/ \langle T_{\mathrm{AA}} \rangle \frac{\mathrm{d}^2 \sigma^{pp}}{\mathrm{d}p_{\mathrm{T}}\mathrm{d}\eta}, \tag{1}$$

[1] ATLAS uses a right-handed coordinate system with its origin at the nominal interaction point (IP) in the centre of the detector and the z-axis along the beam pipe. The x-axis points from the IP to the centre of the LHC ring, and the y-axis points upward. Cylindrical coordinates (r, ϕ) are used in the transverse plane, ϕ being the azimuthal angle around the z-axis. The pseudorapidity is defined in terms of the polar angle θ as $\eta = -\ln\tan(\theta/2)$.

where $\mathrm{d}^2N^{\mathrm{Pb+Pb}}/\mathrm{d}p_{\mathrm{T}}\mathrm{d}\eta$ is the differential jet yield in N_{evt} Pb+Pb events in a given centrality range, $\mathrm{d}^2\sigma^{pp}/\mathrm{d}p_{\mathrm{T}}\mathrm{d}\eta$ is the jet cross-section in pp collisions, and $\langle T_{\mathrm{AA}}\rangle$ can be considered as a luminosity of nucleons per Pb+Pb collision. Therefore, the term in the denominator is the expected yield in Pb+Pb collisions in the absence of any nuclear effects.

In central Pb+Pb collisions, the nuclei collide head on and create a large and long-lived volume of QGP. The developing showers of high-p_{T} partons undergo substantial interactions with the QGP, such that part of their momentum is transfered to large angles relative to the initial parton direction [6, 7]. Therefore, the total momentum in a fixed-size jet cone is decreased compared to the process with analogous initial kinematics occurring in pp collisions, and the jets can be thought of as migrating to lower p_{T} values in Pb+Pb events. Since the jet spectrum is steeply falling with p_{T}, this results in an R_{AA} below unity with a magnitude that depends on the amount of transported energy and the local shape of the spectrum. In central Pb+Pb events at the LHC, the R_{AA} for inclusive jets is suppressed by approximately a factor of two at $p_{\mathrm{T}} \approx 100$ GeV [8–10]. While the R_{AA} is expected to be impacted by other effects, such as the modification of parton densities in the nucleus (nPDFs), these are understood to be modest for inclusive jets and thus most of the signal is due to jet energy loss [11–13].

A key aspect to the theoretical description of jet quenching is its sensitivity to the colour charge of the initiating parton, i.e., whether that parton is a quark or a gluon [14–25]. If the jet-medium interaction is predominantly described as proceeding by radiative emission (medium-induced gluon radiation by strong colour charges), quarks and gluons are generally expected to lose energy in proportion to their QCD colour factors for gluon emission of 4/3 and 3, respectively. Thus, gluon-initiated jets are expected to lose significantly more energy than quark-initiated ones. While the developing parton shower eventually contains both quarks and gluons, theoretical models indicate that the charge of the initiating parton should have a significant impact. At LHC energies, inclusive jet production in the region $p_{\mathrm{T}} < 200$ GeV is dominated by gluon-initiated jets.

Several previous measurements have attempted to explore the colour charge dependence of jet suppression, but with additional effects that may complicate its extraction. For example, Ref. [8] measured jet suppression as a function of jet rapidity, which changes the quark/gluon-initiated jet fraction, but may also sample different regions of the QGP medium [23]. Refs. [26, 27] report the suppression of b-jets, which have a significantly larger quark-initiated fraction than inclusive jets, but have additional effects from the large mass of b-quarks.

An alternative strategy, including the one employed in this Letter, is to measure jets produced in association with an isolated photon or other electroweak (EW) boson, for example through Compton scattering ($gq \rightarrow q\gamma$). These jets are substantially more likely to be initiated by a quark than inclusive jets at the same p_{T}. Importantly, the kinematics of the colourless photon or EW boson are not significantly modified by the QGP [28–31]. Therefore ATLAS has used an isolated photon or Z boson as a way to select partons with a known distribution of initial kinematics before jet quenching [32] and to study how the resulting jet [33] or hadron [34, 35] distributions are modified in particular selections of boson p_{T}, compared to those in pp collisions.

This Letter presents a measurement of the process pp (or NN) $\rightarrow \gamma$+jet+X, as a function of jet p_{T}. Unlike previous measurements mentioned above (Ref. [33–35]), the results in this paper are not normalized per-photon, but measure the full photon-associated jet production cross-section. The measurement is performed using 260 pb^{-1} and 1.7 nb^{-1} of pp and Pb+Pb collisions, respectively, at an NN centre-of-mass energy $\sqrt{s_{\mathrm{NN}}} = 5.02$ TeV recorded with the ATLAS detector at the LHC. Events are required to have an isolated photon with $p_{\mathrm{T}}^{\gamma} > 50$ GeV and $|\eta^{\gamma}| < 2.37$ (excluding the region $1.37 < |\eta^{\gamma}| < 1.52$). At

leading order (LO), the photon isolation requirement predominantly selects direct photons, which are those produced directly in the hard scattering, but also a contribution from fragmentation photons that are radiated in a parton shower after the scattering. All jets with $\left|\eta^{\text{jet}}\right| < 2.8$ and $p_{\text{T}}^{\text{jet}} > 50$ GeV in an opposing azimuthal direction to the photon ($\Delta\phi_{\gamma,\text{jet}} > 7\pi/8$) are included in the measurement. This requirement selects a set of jets with a steeply falling p_{T} distribution, with a large quark-initiated fraction.

The resulting jet production rates in Pb+Pb and pp collisions are used to report R_{AA} and the fractional energy loss quantity, S_{loss}, originally developed by the PHENIX Collaboration at RHIC [36–38] that is conceptually similar to the 'pseudo-quantile' described in Ref. [39]. For a given amount of energy loss, the particular magnitudes of the R_{AA} values are known to depend strongly on the steepness of the pp spectrum. The S_{loss} formulation is designed as an alternative way to characterize the energy loss while removing this dependence. Schematically, S_{loss} is the fractional decrease in $p_{\text{T}}^{\text{jet}}$ at which the $\langle T_{\text{AA}}\rangle$-scaled jet yield in Pb+Pb events reaches the same magnitude as the cross-section in pp events at the original $p_{\text{T}}^{\text{jet}}$. Quantitatively, for each value of the $p_{\text{T}}^{\text{jet}}$ in pp collisions, p_{T}^{pp}, the shift function, $\Delta p_{\text{T}}(p_{\text{T}}^{pp})$, is defined as

$$\Delta p_{\text{T}} = p_{\text{T}}^{pp} - p_{\text{T}}^{\text{Pb+Pb}} \tag{2}$$

where $p_{\text{T}}^{\text{Pb+Pb}}$ is the value for which

$$\frac{1}{\langle T_{\text{AA}}\rangle}\frac{1}{N_{\text{evt}}}\frac{\mathrm{d}^2 N^{\text{Pb+Pb}}\left(p_{\text{T}}^{\text{Pb+Pb}} = p_{\text{T}}^{pp} - \Delta p_{\text{T}}\right)}{\mathrm{d}p_{\text{T}}^{\text{Pb+Pb}}\mathrm{d}\eta} = \frac{\mathrm{d}^2\sigma^{pp}\left(p_{\text{T}}^{pp}\right)}{\mathrm{d}p_{\text{T}}^{pp}\,\mathrm{d}\eta} \times \left[1 + \frac{\mathrm{d}\Delta p_{\text{T}}}{\mathrm{d}p_{\text{T}}^{pp}}\right] \tag{3}$$

where the expression in square brackets is the Jacobian term necessary to, e.g., preserve the total number of jets. The fractional energy loss is given by $S_{\text{loss}}(p_{\text{T}}^{pp}) = \Delta p_{\text{T}}/p_{\text{T}}^{pp}$. It is related to, but not identical to, the average energy lost by jets originating at a given p_{T} in pp collisions, and is a useful way to characterize the magnitude of energy loss in a way that does not depend on the local shape of the spectrum.

The R_{AA} and S_{loss} results for photon-tagged jets are then compared with the analogous ones for inclusive jets [8], whose production in this kinematic range has a significantly smaller quark-initiated fraction. Since the main difference between the jet populations is in their quark and gluon composition, this comparison allows a controlled examination of the impact of the initiating parton's QCD colour charge on jet energy loss.

2 ATLAS detector

The ATLAS detector [40] at the LHC is a multipurpose particle detector with a forward–backward symmetric cylindrical geometry and a near 4π coverage in solid angle. Its inner tracking detector is surrounded by a thin superconducting solenoid providing a 2 T axial magnetic field, and electromagnetic (EM) and hadron calorimeters. The inner tracking detector covers the pseudorapidity range $|\eta| < 2.5$. It consists of silicon pixel, silicon microstrip, and transition radiation tracking detectors. Lead/liquid-argon (LAr) sampling calorimeters provide EM energy measurements with high granularity. A steel/scintillator-tile hadron calorimeter covers the central pseudorapidity range ($|\eta| < 1.7$). The endcap and forward regions are instrumented with LAr calorimeters for both the EM and hadronic energy measurements up to $|\eta| = 4.9$. A zero-degree calorimeter (ZDC) was situated at $|\eta| > 8.3$ during Pb+Pb data-taking. It is composed of alternating layers of quartz rods and tungsten plates and is mostly sensitive to spectator neutrons from fragmenting nuclei in Pb+Pb collisions.

A two-level trigger system is used to select events [41]. The first-level trigger is implemented in hardware and uses a subset of the detector information to accept events at a rate below 100 kHz. This is followed by a software-based trigger that reduces the accepted event rate to 1 kHz on average depending on the data-taking conditions. An extensive software suite [42] is used in data simulation, in the reconstruction and analysis of real and simulated data, in detector operations, and in the trigger and data acquisition systems of the experiment.

3 Event reconstruction

Events were selected using triggers that required a reconstructed photon with p_{T} above 35 GeV (20 GeV) in pp (Pb+Pb) collisions [41, 43]. The trigger sampled the full luminosity corresponding to 260 pb^{-1} of pp data in 2017 and 1.7 nb^{-1} of Pb+Pb data in 2018, and was fully efficient for the photon selection described below. Events are required to satisfy detector and data-quality requirements and, in Pb+Pb collisions, to have a reconstructed vertex.

The Pb+Pb event centrality is characterized by the sum of the transverse energy, $\Sigma E_{\mathrm{T}}^{\mathrm{FCal}}$ in the forward calorimeters, $3.2 < |\eta| < 4.9$. Events in different ranges of $\Sigma E_{\mathrm{T}}^{\mathrm{FCal}}$ are associated with an underlying Pb+Pb collision geometry according to a Monte Carlo (MC) Glauber simulation [5, 44]. This analysis uses three centrality intervals corresponding to the following fractions of the $\Sigma E_{\mathrm{T}}^{\mathrm{FCal}}$ distribution in minimum-bias events: 0–10% ('central' events, with a large nuclear overlap and large $\Sigma E_{\mathrm{T}}^{\mathrm{FCal}}$ values), 10–30%, and 30–80% ('peripheral' events).

Photons are reconstructed following the method used previously in Pb+Pb collisions [28, 33, 35], which applies the procedure used in pp collisions [45] after an event-by-event estimation and subtraction of the underlying event (UE) contribution to the energy deposited in each calorimeter cell [46] (described further below). Photon candidates are required to satisfy 'tight' shower shape requirements designed to reject photons arising from neutral meson decays and from the start of hadronic showers in the EM calorimeter [47]. In pp collisions, photons are further required to be isolated by requiring that the sum of the transverse energy in calorimeter cells within $\Delta R = 0.3$ (not including the contribution from the photon itself) is less than 3 GeV. In Pb+Pb collisions, the UE fluctuations within the isolation cone result in a substantial broadening of the isolation E_{T} distribution. Thus, in Pb+Pb collisions, the isolation energy requirement is centrality dependent and is chosen so that its efficiency for prompt photons is 90%, as determined from simulated events. This upper limit on the isolation energy is approximately 10 GeV in 0–10% Pb+Pb events, but quickly decreases in more peripheral events and converges to the pp value.

Jets are reconstructed following the procedure used in Pb+Pb collisions [8, 46], which is summarized here. Calorimeter cells in all layers are evaluated at the EM energy scale and regrouped into $\Delta\eta \times \Delta\phi = 0.1 \times \pi/32$ logical towers, and the anti-k_t algorithm [48, 49] with parameter $R = 0.4$ is applied to the towers. After the initial jet-finding, the contribution to the energy deposited in towers by the UE is estimated on an event-by-event basis, allowing for the variation of the UE as a function of η and ϕ (the latter arising from the global collective flow in Pb+Pb collisions). Information from towers within $\Delta R = 0.4$ of jet candidates is excluded to avoid biasing the UE estimate. The kinematics of the tower energies are updated to subtract the estimated UE contribution, and the UE procedure is iterated using a better-defined set of jets to define the exclusion regions. The resulting set of jet kinematics is corrected using p_{T}- and η-dependent factors, determined from simulation, to account for the response of the calorimeter to jets [50]. An additional correction for the absolute response in data is based on *in situ* studies of jets recoiling against photons, Z bosons, and jets in other regions of the calorimeter in pp collisions [51]. This calibration is followed by

a 'cross-calibration' that relates the jet energy scale (JES) in high-luminosity 13 TeV pp collisions [52] to the jets reconstructed by the procedure outlined above in the 5.02 TeV data to account for additional differences between the data and simulations.

4 Simulation

Samples of MC-simulated events are used to evaluate the performance of the photon and jet reconstruction and to correct the measured distributions for detector effects. The main MC sample corresponding to photon+jet production in pp data consists of Pythia 8 [53] events, produced with the A14 [54] set of tuned parameters (tune) and the NNPDF 2.3 LO [55] parton distribution function (PDF) set, including direct and fragmentation contributions. As alternatives, photon+jet events were also produced using two additional generators. The Sherpa 2.2.4 [56, 57] generator was run at next-to-leading order (NLO) with the NNPDF 3.0 NNLO [58] PDF set to produce a sample of events containing a photon plus up to three other partons. The Herwig 7.2 [59] generator was run at leading order with the MMHT2014lo [60] PDF set, with separate samples produced for direct and fragmentation photons. The three sets of events were simulated [42] using a Geant4 [61] description of the ATLAS detector and were digitized and reconstructed in a manner identical to that of the data. The generator-level final state photons in the MC samples are required to be isolated by requiring that the sum of the transverse energy of all the final state particles, excluding the photon itself, within a $\Delta R = 0.4$ cone is less than 5 GeV.

The fraction of quark-initiated jets, as defined in simulation in Ref. [62], is estimated by using three different MC generators (Pythia 8, Herwig and Sherpa) for the photon-tagged jets, and is compared with that for inclusive jets [8] in Figure 1. The generators predict that 75–80% of all photon-tagged jets at $p_{\mathrm{T}}^{\mathrm{jet}} = 50$ GeV are initiated by quarks, while this is true for only 30–40% of inclusive jets at the same $p_{\mathrm{T}}^{\mathrm{jet}}$. At higher $p_{\mathrm{T}}^{\mathrm{jet}}$, the quark-initiated fractions for photon-tagged and inclusive jets slowly fall and rise, respectively, reaching 50–60% for both samples at 300 GeV. Thus, according to the MC generators, these two samples contain significantly different quark-initiated jet fractions with $p_{\mathrm{T}}^{\mathrm{jet}} \lesssim 200$ GeV.

To simulate photon+jet events in Pb+Pb data, the events described above were overlaid at the detector-hit level with a sample of Pb+Pb data events recorded with minimum-bias and central-event triggers. The combination of the simulated and data event was then reconstructed as a single event. These 'Pb+Pb data overlay' events are re-weighted to match the observed $\Sigma E_{\mathrm{T}}^{\mathrm{FCal}}$ distribution for photon+jet events in Pb+Pb data. In this way, the features of the Pb+Pb UE in the simulated samples are identical to those in real Pb+Pb data.

Finally, to evaluate the possible impact of nuclear effects, such as the modification of PDFs on the measurement, samples of generator-level Pythia 8 events were produced for photon+jet and inclusive jet events, again including both direct and fragmentation photons and the generator-level isolation requirement. For both of these processes, separate samples were generated for pp, proton–neutron (pn), and neutron–neutron (nn) events, and the cross-section in simulated Pb+Pb events was constructed via a weighted sum $\left(Z^2\sigma^{pp} + 2Z(A-Z)\sigma^{pn} + (A-Z)^2\sigma^{nn}\right)/A^2$, where A and Z are the mass and atomic number of Pb, respectively. In a separate procedure, the cross-section in the pp samples was evaluated after being weighted on an event-by-event basis with the central values of the EPPS16 nPDF set [63], at NLO and configured for the lead nucleus with the grid file EPPS16NLOR_208.

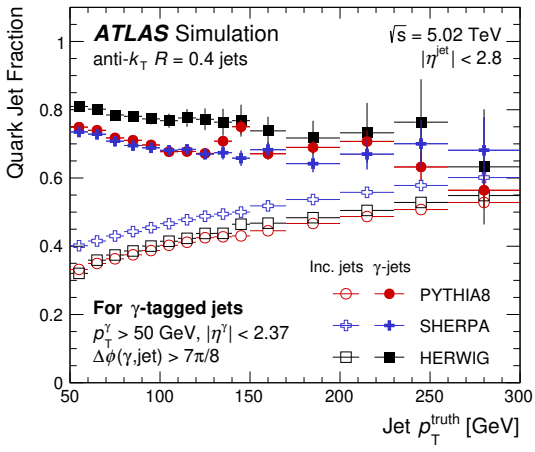

Figure 1: Fraction of photon-tagged jets (filled markers) and inclusive jets (open markers) initiated by a quark, as a function of generator-level $p_{\mathrm{T}}^{\mathrm{jet}}$, in the Pythia 8 (circles), Herwig (squares), and Sherpa (crosses) event generators. The vertical bars associated with symbols indicate the statistical uncertainties.

5 Analysis

The signal definition for this measurement is $R = 0.4$ jets with $p_{\mathrm{T}}^{\mathrm{jet}} > 50$ GeV that are $\Delta\phi_{\gamma,\mathrm{jet}} > 7\pi/8$ from a $p_{\mathrm{T}}^{\gamma} > 50$ GeV isolated photon, with all candidate jets in a given event included in the measurement. The two-dimensional yield $(p_{\mathrm{T}}^{\gamma}, p_{\mathrm{T}}^{\mathrm{jet}})$ is constructed for photons and their associated jets, but using thresholds of 40 GeV on the photon and jet p_{T}, to allow for the correction of bin migration effects (discussed below).

Figure 2 shows the signal $p_{\mathrm{T}}^{\mathrm{jet}}/p_{\mathrm{T}}^{\gamma}$ distributions in pp data at the reconstructed-level (i.e., without any of the corrections for photon purity, efficiency, and unfolding described below), compared with the same in simulated Pythia 8 events. The contributions from direct and fragmentation photons in Pythia 8 are shown separately as shaded histograms, with the former contribution peaking near unity due to the back-to-back kinematics, and the latter distribution extending to large $p_{\mathrm{T}}^{\mathrm{jet}}/p_{\mathrm{T}}^{\gamma}$ values. At the lowest $p_{\mathrm{T}}^{\mathrm{jet}}$ bin of $50 < p_{\mathrm{T}}^{\mathrm{jet}} < 60$ GeV, the $p_{\mathrm{T}}^{\mathrm{jet}}/p_{\mathrm{T}}^{\gamma}$ distribution in data has no entries above 1.2 because of the kinematic selection on the photons ($p_{\mathrm{T}}^{\gamma} > 50$ GeV), and thus the comparison with simulation suggests that direct photons are dominant. However, at high $p_{\mathrm{T}}^{\mathrm{jet}}$ values (e.g., in the right most panel), there is a growing contribution from fragmentation photons, which may contribute to the decreasing quark-initiated jet fraction in Figure 1.

Notably, Pythia 8 does not precisely match the $p_{\mathrm{T}}^{\mathrm{jet}}/p_{\mathrm{T}}^{\gamma}$ distribution in data, in particular over-estimating the relative magnitude of the fragmentation photon contribution. A similar conclusion was reached in the study of photon+jet events in pp collisions at 7 TeV [64], where Pythia 8 better describes the data after an increased (decreased) weighting of the direct (fragmentation) contributions in that generator. While this exercise is not repeated in this measurement, the dashed line in Figure 2 indicates how de-weighting the fragmentation photon contribution in Pythia 8 by, e.g., a factor of two would modify the jet p_{T} distribution in that generator. Therefore this study highlights the need for the pp baseline in theoretical calculations of jet quenching to properly model the relative direct and fragmentation photon contributions in photon+jet processes.

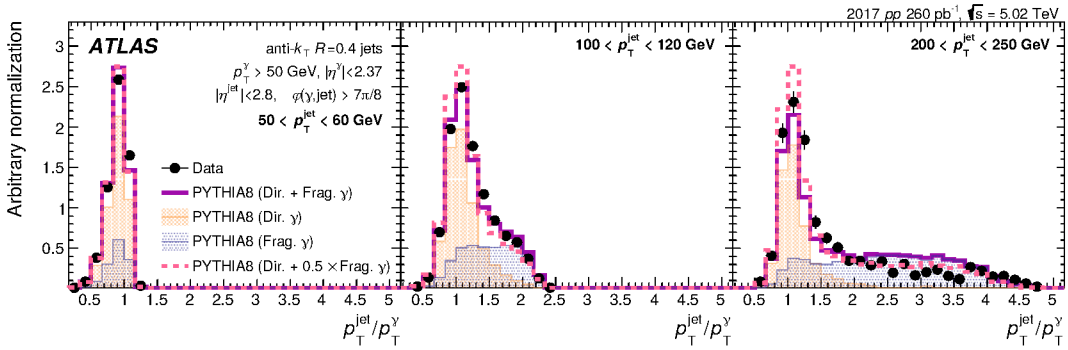

Figure 2: Reconstructed-level $p_{\mathrm{T}}^{\mathrm{jet}}/p_{\mathrm{T}}^{\gamma}$ distributions for different $p_{\mathrm{T}}^{\mathrm{jet}}$ bins: (left panel) $50 < p_{\mathrm{T}}^{\mathrm{jet}} < 60$ GeV (middle panel) $100 < p_{\mathrm{T}}^{\mathrm{jet}} < 120$ GeV and (right panel) $200 < p_{\mathrm{T}}^{\mathrm{jet}} < 250$ GeV for $p_{\mathrm{T}}^{\gamma} > 50$ GeV. The data (filled circles) is compared with reconstructed-level Pythia 8 (solid line), which is normalized to the data. The shaded histograms show the breakdown of Pythia 8 contributions from photon-production processes: direct (checkered hatching) and fragmentation (dashed hatching) photons. The dashed-line histogram represents Pythia 8 events, including all direct photon events with the fragmentation photon events scaled down by a factor of two.

The initial $(p_{\mathrm{T}}^{\gamma}, p_{\mathrm{T}}^{\mathrm{jet}})$ yield in Pb+Pb collisions contains jets that do not arise from the same hard scattering as the photon, but rather from an unrelated NN scattering, or from jets that are reconstructed from the localized fluctuations of the UE. This combinatoric contribution is estimated through a 'mixing' technique in which high-p_{T} photons in data are correlated with jets in minimum-bias Pb+Pb events that match the overall properties of the original, photon-containing event. These matched properties include the $\Sigma E_{\mathrm{T}}^{\mathrm{FCal}}$ and flow plane angle. The resulting combinatoric jet contribution is observed to be flat in $\Delta\phi$, as expected for unrelated pairs. For the lowest $p_{\mathrm{T}}^{\mathrm{jet}}$ values in the most central events, the background contribution is approximately half of the total yield, but this fraction falls very rapidly with increasing $p_{\mathrm{T}}^{\mathrm{jet}}$ or in less central events. The contribution is statistically subtracted from the initial yields.

Even after the photon identification and isolation conditions above are applied to data, the selected photons still include a considerable contribution from backgrounds, dominantly from neutral hadron decays (e.g., $\pi^0, \eta \to \gamma\gamma$). These decay photons may be reconstructed as a single cluster that satisfies the 'tight' identification and the isolation conditions. Thus, the photon-associated jet yields contain a contribution from, e.g., π^0-associated jet yields. To correct for this, the purity of prompt, isolated photons in the selected data sample is determined by using a data-driven, double-sideband method widely used in ATLAS photon measurements [65–68], separately for each selection in event centrality and p_{T}^{γ}. The purity has a minimum of $\approx 75\%$ in central Pb+Pb events at the lowest p_{T}^{γ} values, but then increases rapidly with p_{T}^{γ} and in more peripheral Pb+Pb or pp events to a plateau of $\approx 95\%$. The shape of the $p_{\mathrm{T}}^{\mathrm{jet}}$ contribution from this background is determined by performing the same analysis but using an inverted signal selection on the photon. This selection requires the photon to still be isolated, but fail to satisfy several shower shape requirements in a way that is designed to greatly enhance the neutral hadron background. Finally, the background level is scaled according to the purity in each p_{T}^{γ} and centrality selection, and statistically subtracted from the yields.

To correct for the bin-to-bin migration in the p_{T}^{γ} and $p_{\mathrm{T}}^{\mathrm{jet}}$ distributions arising from the finite detector resolution and residual defects in the JES, a two-dimensional unfolding procedure on the background-subtracted $(p_{\mathrm{T}}^{\gamma}, p_{\mathrm{T}}^{\mathrm{jet}})$ yields is used. The Pythia 8 simulation samples are used to generate independent

response matrices for *pp* events and for each centrality range in Pb+Pb events, after reweighting the $p_{\mathrm{T}}^{\mathrm{jet}}$ distributions in simulation to match those measured in data. The iterative Bayesian method [69] is used with the RooUnfold software package [70]. The number of iterations used in the unfolding is determined by minimizing the sum in quadrature of the total statistical uncertainty and the differences in the unfolded distribution between consecutive iterations. This number is two or three depending on the event centrality. The unfolding procedure also accounts for the finite reconstruction and selection efficiency for photons, which is $\approx 70\%$ at low-p_{T}^{γ} in central Pb+Pb events, but rises rapidly with p_{T}^{γ} and in more peripheral events to a plateau of $\approx 85\%$, and for a small inefficiency for jets at low $p_{\mathrm{T}}^{\mathrm{jet}}$. When tested in simulation, this unfolding procedure leads to a recovery of the original generator-level distribution within the statistical uncertainties of the test sample.

6 Systematic uncertainties

The main sources of systematic uncertainty in this measurement are those associated with the photon, jet, and unfolding components. For most of the sources described below, the entire analysis is repeated with a given variation, and the change in the results is taken as the corresponding uncertainty. These individual uncertainties are treated as independent and added in quadrature to quantify the full uncertainties.

The photon measurement includes several uncertainty components. First, the reconstructed energy of photons in simulation is varied according to the uncertainties in the photon energy scale and resolution [71]. Second, the reconstructed shower shape variables used to identify photons are varied in simulation [47]. Third, the isolation and identification sideband boundaries used in purity determination are varied in a manner similar to that in Refs. [33, 35]. Fourth, the difference between using the nominal purity values and the results of a smooth fit to those values is considered. Finally, the reconstruction-level isolation energy requirement is varied such that isolation efficiency for signal photons is 85% and 95%, instead of the nominal 90%. These variations result in different estimates of the photon purity, and thus test the stability of the extracted yield to any potentially imperfect description of photon isolation energy distributions in simulations. The uncertainty in the yields from all these sources is typically 3–6% in *pp* collisions (4–15% in central Pb+Pb collisions), rising with jet p_{T}.

For the jet-related uncertainties, the reconstructed jet energy in simulation is varied according to the uncertainties in the JES and jet energy resolution (JER). As in other Run 2 heavy-ion jet measurements [8, 33, 35, 72], the JES uncertainties have four main components. First, a centrality-independent baseline component determined from *in situ* studies of the calorimeter response to jets reconstructed following the procedure used in 13 TeV *pp* collisions [51, 73]. Second, a centrality-independent component accounting for the relative energy scale difference between the heavy-ion jet reconstruction in this analysis and that used for 13 TeV *pp* collisions [52]. Third, a component that accounts for potential inaccuracies in the relative abundances of jets initiated by quarks and gluons, and of their different calorimetric response, in simulation. This uncertainty was evaluated by using the flavour fractions and flavour-dependent response in the Herwig, instead of Pythia 8, simulation samples. Finally, a centrality-dependent component accounting for a different structure and possibly a different detector response of jets in Pb+Pb collisions that is not modelled in simulation. This uncertainty is determined by the method used for 2015 and 2011 data [52] that compares the calorimeter $p_{\mathrm{T}}^{\mathrm{jet}}$ with the p_{T} sum of the charged particles in the jets in data and simulation. For the JER uncertainty, the reconstructed $p_{\mathrm{T}}^{\mathrm{jet}}$ in simulation is smeared by a factor evaluated using an *in situ* technique in 13 TeV *pp* data [74, 75], and by an additional contribution to account for the differences between the heavy-ion jet reconstruction and that in the 13 TeV *pp* data. The JES and

JER uncertainties in the jet yields are typically 3–7% in pp collisions, rising slowly with jet p_{T}, and are modestly higher in Pb+Pb collisions due to the final uncertainty source described above.

Two uncertainties associated with the unfolding procedure are evaluated. First, the impact of a different prior in the response matrices was determined by not applying the reweighting factors to account for the difference in the distributions between data and simulation. These were at most 5% at low $p_{\mathrm{T}}^{\mathrm{jet}}$, decreasing to 1% at high $p_{\mathrm{T}}^{\mathrm{jet}}$. Second, a resampling study is used to determine the impact on the results from the limited size of the simulated samples. These are included as part of the statistical uncertainties, but they are typically much smaller than the statistical uncertainties in data.

The mixed event technique was tested in the simulation samples, where the combinatoric contribution is exactly known. Any "non-closure" in the procedure (i.e. failure to fully subtract the combinatoric contribution) is considered as a source of uncertainty. Finally, there are uncertainties in the overall normalization of the measurements. For the pp cross-section, these arise from the luminosity of the pp data and are estimated to be 1.6% using the beam separation scan analysis methods similar to that in Ref. [76]. For the $1/\langle T_{\mathrm{AA}}\rangle$-scaled yields in Pb+Pb collisions, the uncertainties are determined by adjusting the parameters in the Glauber analysis [5, 44], and vary from 0.5% to 2.8% in central to peripheral collisions, respectively.

Uncertainty sources that are correlated between Pb+Pb and pp collisions, which include most of the jet- and photon-related uncertainties, typically cancel out to a large degree in R_{AA}. The most significant uncorrelated uncertainties are the centrality-dependent JES and unfolding ones.

For both the cross-section and R_{AA} measurements, the unfolding (photon purity) uncertainties are dominant at $p_{\mathrm{T}}^{\mathrm{jet}} < 80$ GeV for the 0–10% and 10–30% centrality intervals (30–80% centrality interval and in pp collisions). At $80 < p_{\mathrm{T}}^{\mathrm{jet}} < 200$ GeV, the JES, JER and photon purity uncertainties are dominant in all centrality bins and in pp collisions. The photon isolation uncertainties are dominant at $p_{\mathrm{T}}^{\mathrm{jet}} > 200$ GeV in all centrality bins and in pp collisions. In comparisons of the value of R_{AA} reported in this paper to that measured for inclusive jets [8], the uncertainties in the two measurements are treated as uncorrelated. For the S_{loss} analysis, these uncertainties are propagated as part of the S_{loss} determination procedure, described below in Section 8.1.

7 Results

Figure 3 shows the measured cross-section for photon-tagged jet production in pp collisions, compared with the same quantity in the Pythia 8, Herwig, and Sherpa event generators. The distributions of the generators are normalized to have the same total cross-sections as the data. The data is best described by Herwig, which has a shape compatible with the data within its uncertainties over the entire measured $p_{\mathrm{T}}^{\mathrm{jet}}$ range. Pythia 8 and Sherpa are compatible with the data in the low $p_{\mathrm{T}}^{\mathrm{jet}}$ region ($p_{\mathrm{T}}^{\mathrm{jet}} < 100$ GeV) but have a higher relative cross-section than the data at higher $p_{\mathrm{T}}^{\mathrm{jet}}$. The level of agreement between the MC generators and the data has a similar magnitude and p_{T} dependence as that observed in previous measurements in pp collisions at 7 TeV [64].

Figure 4 shows the $\langle T_{\mathrm{AA}}\rangle$-scaled photon-tagged jet yields for different centrality bins in Pb+Pb collisions and the cross-section in pp collisions. The ratio of cross-sections for photon-tagged jets to that for inclusive jets in pp collisions is shown in the bottom panel. Both the pp inclusive jet and photon-tagged jet cross-sections are steeply falling as a function of $p_{\mathrm{T}}^{\mathrm{jet}}$, but the photon-tagged jet cross-section has a

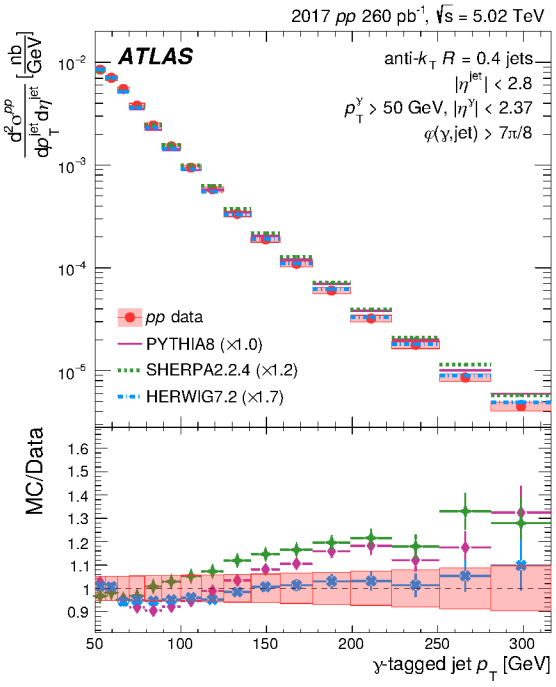

Figure 3: Top panel: The differential cross-section of photon-tagged jets as a function of $p_{\mathrm{T}}^{\mathrm{jet}}$ in pp data, compared with that in PYTHIA 8 (solid line), SHERPA 2.2.4 (dotted line) and HERWIG 7.2 (dash-dotted line) MC samples. The statistical uncertainties in the data are small and hidden by the symbols, and are drawn as vertical bars for the MC samples. The total systematic uncertainties in the data are shown as boxes in each $p_{\mathrm{T}}^{\mathrm{jet}}$ bin. The MC distributions are normalized using the factors shown in parentheses to have the same total cross-sections as the data. Bottom panel: The ratio of cross-sections from different MC generators to the data.

less steep spectrum, i.e., it decreases more slowly with $p_{\mathrm{T}}^{\mathrm{jet}}$. As described above, the R_{AA} depends on the convolution of the energy loss due to jet quenching with the slope of the $p_{\mathrm{T}}^{\mathrm{jet}}$ spectrum and this must be taken into account when comparing results between inclusive and photon-tagged jets.

The R_{AA} values of photon-tagged jets are computed according to Eq. (1) above, and are shown in Figure 5 as a function of $p_{\mathrm{T}}^{\mathrm{jet}}$ in different centrality intervals. In 0–10% Pb+Pb collisions, the R_{AA} for photon-tagged jets is suppressed below unity, as expected from jet energy loss, at the level of 0.25–0.40. Below 70 GeV, as the jet p_{T} decreases, the R_{AA} values systematically increase. As the R_{AA} depends not only on the energy loss but on the local shape of the initial spectrum, this increase may be related to the flattening of the spectrum near $p_{\mathrm{T}}^{\mathrm{jet}} = 50$ GeV, which is caused by the kinematic selection $p_{\mathrm{T}}^{\gamma} > 50$ GeV. In the region $p_{\mathrm{T}}^{\mathrm{jet}} < 200$ GeV, the R_{AA} is found to be larger in the 30–80% Pb+Pb collisions than in the 0–10% Pb+Pb collisions, indicating more suppression in central Pb+Pb collisions as expected due to a larger jet quenching effect in collisions with a larger volume and higher temperature QGP.

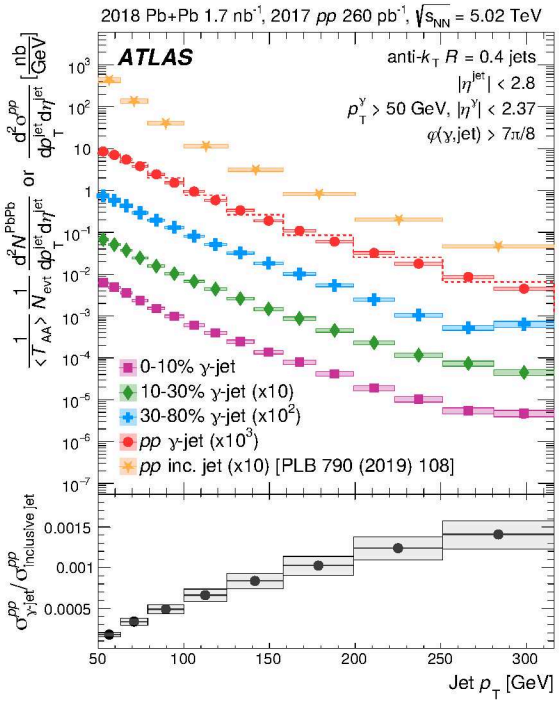

Figure 4: Top panel: The yields of photon-tagged jets as a function of $p_{\mathrm{T}}^{\mathrm{jet}}$ in Pb+Pb events for 0–10% (squares), 10–30% (diamonds) and 30–80% (crosses) centrality bins and the differential cross-section in pp events (circles). The spectra are scaled by the factors shown in the legend for clarity. The inclusive jet cross-section in pp collisions [8] (stars) is shown for comparison. The statistical uncertainties are small and hidden by the symbols. The total systematic uncertainties are shown as boxes in each $p_{\mathrm{T}}^{\mathrm{jet}}$ bin. The photon-tagged jet pp data is also re-binned to match the binning of inclusive jet data (shown as dotted line). Bottom panel: The ratio of cross-sections between photon-tagged jets and inclusive jets in pp collisions. The boxes associated with the data points represent the sum in quadrature of the systematic uncertainties for photon-tagged jets and inclusive jets.

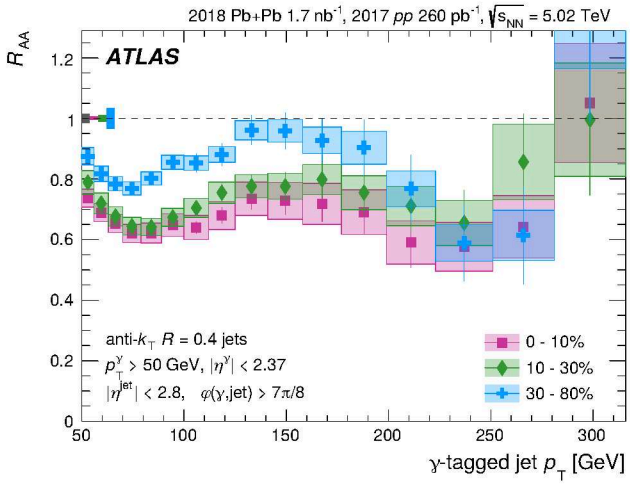

Figure 5: The R_{AA} of photon-tagged jets as a function of $p_{\mathrm{T}}^{\mathrm{jet}}$ for 0–10%, 10–30%, and 30–80% centrality intervals. The vertical bars associated with symbols indicate the statistical uncertainties. The total systematic uncertainties are shown as boxes in each $p_{\mathrm{T}}^{\mathrm{jet}}$ bin. The shaded bars on the left of the axis at $R_{\mathrm{AA}} = 1$ indicate the p_{T}-independent uncertainties associated with the luminosity in pp collisions and $\langle T_{\mathrm{AA}} \rangle$ for 0–10%, 10–30%, and 30–80% Pb+Pb collisions, respectively. The highest $p_{\mathrm{T}}^{\mathrm{jet}}$ data point in the 30–80% centrality interval is 1.42 ± 0.43 (stat.) ± 0.25 (syst.) and extends off the vertical scale.

8 Discussion

Figure 6 compares the photon-tagged jet R_{AA} results to the previously published ATLAS inclusive jet results [8]. The R_{AA} of photon-tagged jets is significantly higher than the corresponding values for inclusive jets for $p_{\mathrm{T}}^{\mathrm{jet}} < 200$ GeV. For $p_{\mathrm{T}}^{\mathrm{jet}} > 200$ GeV, the statistical and systematic uncertainties in the photon-tagged jet results are larger and the two sets of R_{AA} values become compatible.

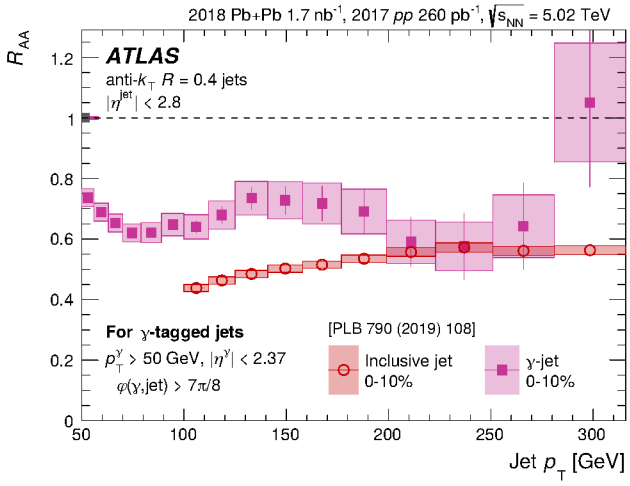

Figure 6: The R_{AA} of photon-tagged jets (filled squares) as a function of $p_{\mathrm{T}}^{\mathrm{jet}}$ for 0–10% Pb+Pb events are overlaid with that of inclusive jets [8] (open circles) in the same centrality range for comparison. The vertical bars associated with symbols indicate the statistical uncertainties. The total systematic uncertainties are shown as boxes in each $p_{\mathrm{T}}^{\mathrm{jet}}$ bin. The shaded bars on the left of the axis at $R_{\mathrm{AA}} = 1$ indicate the p_{T}-independent uncertainties associated with the luminosity in pp collisions and $\langle T_{\mathrm{AA}} \rangle$ for 0–10% Pb+Pb collisions, respectively.

A primary goal of this measurement is to isolate the effect of colour charge on jet quenching. Indeed, in the range of $p_{\mathrm{T}}^{\mathrm{jet}}$ where the quark-initiated fraction is significantly higher in photon-tagged jets (see Figure 1), the R_{AA} is significantly higher than that for inclusive jets. However, the R_{AA} is known to depend on the shape of the initial production spectrum with, e.g., a steeper spectrum resulting in a lower R_{AA} for the same magnitude of energy loss. Indeed, Figure 4 shows that although the jet p_{T} spectra for photon-tagged and inclusive jets are both steeply falling, the latter is systematically steeper than the former. Thus, it is important for theoretical calculations attempting to describe the R_{AA} results to first correctly describe the photon-tagged and inclusive jet cross-sections in pp collisions, i.e., before applying any jet quenching.

8.1 Fractional energy loss analysis

An alternative way to characterize the energy loss with a greatly reduced sensitivity to the spectral shape is through the fractional energy loss quantity, S_{loss}, introduced in Section 1.

To determine S_{loss} for the photon-tagged jet case, the distributions in pp and Pb+Pb collisions are fit using the 'extended power law' function introduced in Ref. [14], $f(p_{\mathrm{T}}) = A(p_{\mathrm{T},0}/p_{\mathrm{T}})^{n+\beta \log(p_{\mathrm{T}}/p_{\mathrm{T},0})}$, in the region $p_{\mathrm{T}} > 100$ GeV. An initial estimate of Δp_{T} in Eq. (2) is performed by first assuming that the Jacobian term in Eq. 3, $\left(1 + \mathrm{d}\Delta p_{\mathrm{T}}/\mathrm{d}p_{\mathrm{T}}^{pp}\right)$, is unity, i.e. $\mathrm{d}\Delta p_{\mathrm{T}}/\mathrm{d}p_{\mathrm{T}}^{pp} = 0$, and determining $\Delta p_{\mathrm{T}}(p_{\mathrm{T}}^{pp})$ from the fitted

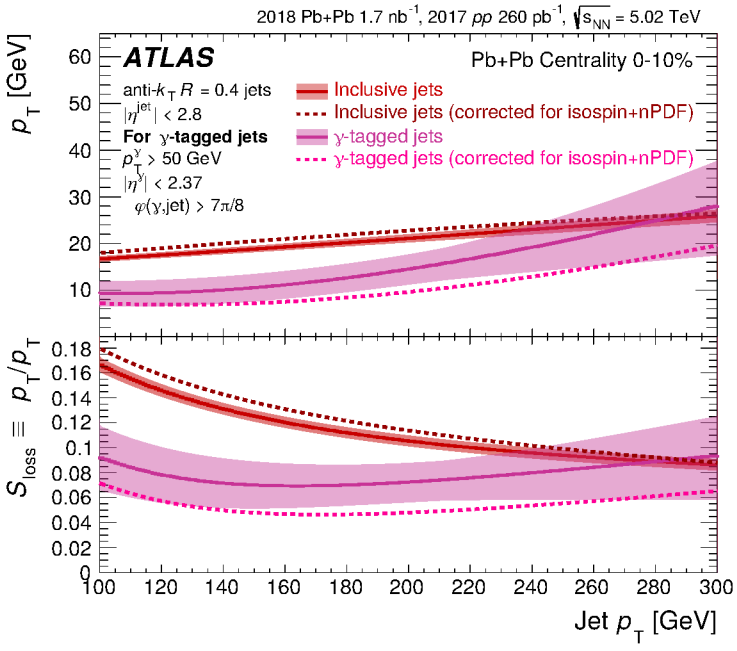

Figure 7: Top panel: The energy loss Δp_{T} as a function of $p_{\mathrm{T}}^{\mathrm{jet}}$ for photon-tagged jets (lower bands) and inclusive jets (upper bands) for the 0–10% centrality interval. The bands around the solid lines indicate the systematic uncertainties. The dashed lines show the updated estimate of Δp_{T} when the data are corrected for isospin and nPDF effects (see text). Bottom panel: The fractional energy loss S_{loss}.

functions. This estimate is then iteratively improved by applying the Jacobian factor to the pp spectrum and repeating the procedure to obtain an updated estimate of Δp_{T}. To determine the systematic uncertainty in Δp_{T}, and thus S_{loss}, the procedure is performed separately under each of the systematic variations detailed in Section 6, with the variations from sources that are correlated between pp and Pb+Pb applied to both distributions simultaneously. An additional uncertainty is assigned to account for the sensitivity of the extracted S_{loss} values to the choice of fit range.

To determine S_{loss} for the inclusive jet case, this procedure is repeated with two modifications. First, to provide a better description of the data, the fit function for the inclusive jet distributions includes an additional term in the exponent that is linear in p_{T}. Second, an alternative procedure is used to account for the correlated uncertainties between the pp and Pb+Pb distributions. The $\langle T_{\mathrm{AA}} \rangle$-scaled Pb+Pb yields are re-calculated by taking the R_{AA} values (including their uncertainties, which account for the correlation between pp and Pb+Pb) and multiplying them by the central values of the pp cross-section. Then, the uncertainties in Δp_{T}, and thus in S_{loss}, are calculated by propagating the uncertainty in the determined value of $p_{\mathrm{T}}^{\mathrm{Pb+Pb}}$ using Eq. (2).

The extracted Δp_{T} and S_{loss} values are shown in Figure 7 for photon-tagged jets and inclusive jets for the 0–10% centrality interval. For photon-tagged jets, Δp_{T} ranges from 10–30 GeV, and S_{loss} from 0.07–0.10. For both samples, Δp_{T} increases with jet p_{T}. In the inclusive jet case, this increase is slower than the jet p_{T}, resulting in S_{loss} values that instead decrease systematically with increasing p_{T}. For the photon-tagged jet case, the S_{loss} values are approximately constant within uncertainties over this $p_{\mathrm{T}}^{\mathrm{jet}}$ range. In the region $100 < p_{\mathrm{T}}^{\mathrm{jet}} \lesssim 200$ GeV, the S_{loss} values for photon-tagged jets are significantly smaller than those for

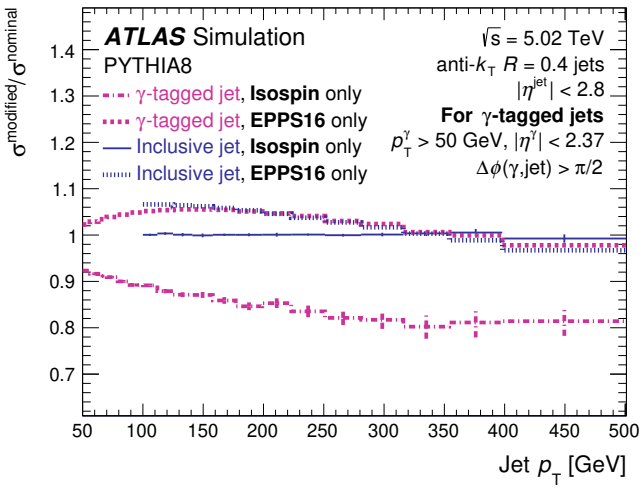

Figure 8: PYTHIA 8-based evaluation of the impact of the isospin and nPDF effects for the two jet samples, shown as the ratio of the modified cross-section to the nominal one in *pp* collisions. The isospin (nPDF) effect for inclusive jets is shown as a solid (dotted) line, and for photon-tagged jets as dot-dashed (dashed) line.

inclusive jets, again suggesting a significant colour-charge dependence to jet energy loss. At higher $p_{\mathrm{T}}^{\mathrm{jet}}$, the two S_{loss} curves are compatible within uncertainties, potentially due to the quark fractions of the two samples becoming more similar in this p_{T} region (Figure 1).

Importantly, $S_{\mathrm{loss}}(p_{\mathrm{T}})$ should not be interpreted as the fraction of the energy lost in the QGP for jets that emerge with the given p_{T} in Pb+Pb collisions. As detailed in Refs. [37, 38], this extracted value is smaller than the true average energy loss. This is due to the steeply falling p_{T} spectrum and jet-to-jet fluctuations in the energy loss, which result in the fact that jets observed in Pb+Pb at a given p_{T} are more likely to be those with smaller than average energy loss. Nevertheless, the procedure above is clearly defined and is a useful way to quantify the difference in the magnitude of energy loss between different scenarios.

Even though the determination of S_{loss} is not strongly sensitive to the initial $p_{\mathrm{T}}^{\mathrm{jet}}$ shape in *pp* collisions, there are other effects that modify the jet spectra in Pb+Pb collisions compared to those in *pp* collisions, which do not arise from energy loss but may impact the extracted S_{loss} values. These include effects originating from isospin (i.e., the different up- and down-quark composition of the nucleus compared to the proton, which decreases the rate of processes such as photon+jet production, as previously observed in *p*+Pb collisions [77]) and the modification of the PDFs in nuclei compared to those in free nucleons.

The possible quantitative impact of these effects can be explored using the generator-level simulation samples described at the end of Section 4. To determine the impact of the isospin and nPDF effects, the simulated cross-section in Pb+Pb events or in nPDF-weighted *pp* events, respectively, was compared with that in the original sample of *pp* events. The ratios of these modified cross-sections to the cross-section in *pp* collisions are shown in Figure 8 separately for photon-tagged and inclusive jets. While the isospin effect for inclusive jets is negligible, it causes the photon-tagged jet spectrum (and thus R_{AA}) in Pb+Pb collisions to decrease by 10–20% in the $p_{\mathrm{T}}^{\mathrm{jet}}$ range of 100–300 GeV. The isospin effect is stronger at larger $p_{\mathrm{T}}^{\mathrm{jet}}$ as the parton in the nucleus involved in the parton–parton scattering is more likely to come from a valence (up/down) quark at large Bjorken-*x* range. The nPDF effects on the photon-tagged and inclusive

jet R_{AA} are similar, leading to approximately a 5% enhancement at 100 GeV (an increase in the nuclear parton densities in the 'anti-shadowing' region) that then decreases with increasing p_{T}. Given the similar nPDF effects, it can be seen that the isospin effect for photon-tagged jets has the dominant impact in the comparisons. It decreases the photon-tagged jet yield in Pb+Pb events, thus causing an overestimate of the energy loss effects under the naive interpretation of S_{loss} and R_{AA}.

To test the potential impact of these effects on the S_{loss} results, the energy loss study is repeated after dividing the measured R_{AA} values by the simulation-derived values in Figure 8 to approximately correct for these effects. The updated S_{loss} values are shown as dashed lines in Figure 7. It can be seen that the differences in energy loss between photon-tagged jets and inclusive jets becomes even larger after accounting for the isospin and nPDF effects, further strengthening the evidence that quark-initiated jets lose less energy than gluon-initiated ones.

8.2 Theoretical comparisons

The R_{AA} results are compared with theoretical calculations of jet energy loss in the QGP that model the colour-charge dependence of the parton-QGP interaction in various ways. As discussed above, it is important for such calculations to properly model details such as the photon production processes (i.e., including fragmentation photons), the spectral shape, and the impact of the isospin and nPDF for a consistent comparison with the data. The five calculations described below typically meet most but not necessarily all these criteria.

The calculation from Takacs *et al.* [15, 16] includes a resummation of energy loss effects from hard, vacuum-like emissions occurring in the medium and the modelling of soft energy flow and recovery at the jet cone. The Takacs *et al.* calculations are presented with a range of the jet-medium coupling parameter $g_{\mathrm{med}} = 2.2$–2.3. The predictions in Refs. [17, 18] are based on a linearised Boltzmann equation with diffusion model (LIDO). The LIDO calculations are presented with a range of values for the parameter $\mu = 1.3\pi T$–$1.8\pi T$, where T is the medium temperature and μ controls the strength of the parton coupling to the medium. The predictions labelled SCET$_{\mathrm{G}}$ [20–22] are based on a Langevin transport model including both collisional and radiative energy losses. The SCET$_{\mathrm{G}}$ calculations are presented with a range of the jet-medium coupling $g = 1.8$–2.2. The CoLBT predictions [23] are a linear Boltzmann transport (LBT) model, which includes elastic and inelastic processes based on perturbative QCD for both jet shower and recoil medium partons as they propagate through a QGP. JEWEL is a MC event generator that simulates QCD jet evolution in heavy-ion collisions, including radiative and elastic energy loss processes, and is configured to include medium recoils [78].

The left and middle panels of Figure 9 show the R_{AA} of photon-tagged jets and inclusive jets, respectively, in 0–10% central Pb+Pb collisions compared with the theoretical predictions. The ratio $R_{\mathrm{AA}}^{\gamma-\mathrm{jet}}/R_{\mathrm{AA}}^{\text{inclusive jet}}$ is shown in the right panel, which in the theoretical predictions leads to the cancellation of some uncertainties common to both R_{AA} calculations. The inclusive jet R_{AA}, a commonly used benchmark to fix free parameters in theoretical models, is well described by all of the calculations. All the calculations except JEWEL qualitatively predict that the photon-tagged jet R_{AA} should be closer to unity than the inclusive jet R_{AA}, but the specific magnitude as a function of $p_{\mathrm{T}}^{\mathrm{jet}}$ varies. The photon-tagged jet R_{AA} data points are generally larger than the central values of many of the calculations, but they are compatible with the CoLBT model and with the calculations by Takacs *et al.* and SCET$_{\mathrm{G}}$ within the range of their respective model parameters. Notably, several of the models predict the increase of the photon-tagged jet R_{AA} with decreasing $p_{\mathrm{T}}^{\mathrm{jet}}$ observed in data at $p_{\mathrm{T}}^{\mathrm{jet}} \lesssim 80$ GeV. The models further predict that the $R_{\mathrm{AA}}^{\gamma-\mathrm{jet}}/R_{\mathrm{AA}}^{\text{inclusive jet}}$

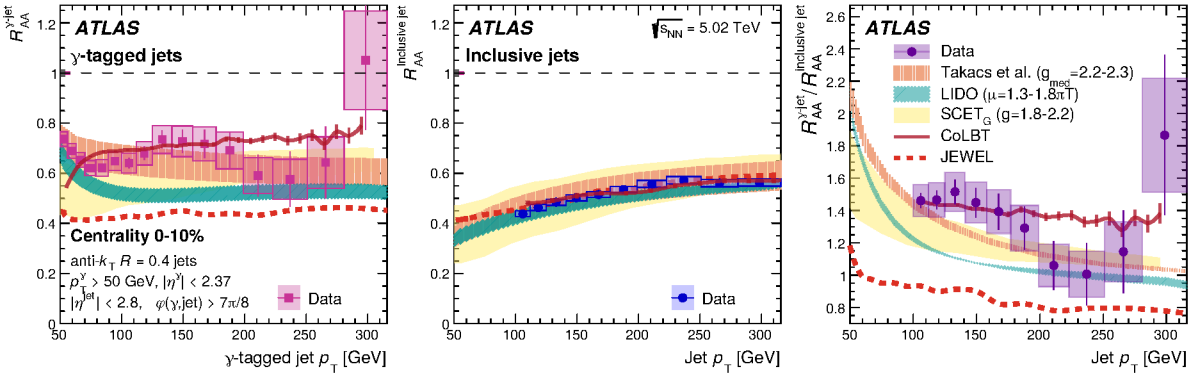

Figure 9: Comparison of R_{AA} between data and various theoretical predictions for (left panel) photon-tagged jets and (middle panel) inclusive jets. The right panel shows $R_{\mathrm{AA}}^{\gamma-\mathrm{jet}}/R_{\mathrm{AA}}^{\mathrm{inclusive\ jet}}$ compared between data and theory predictions. The vertical bars associated with symbols of the photon-tagged jet data indicate the statistical uncertainties and the total systematic uncertainties are shown as boxes in each $p_{\mathrm{T}}^{\mathrm{jet}}$ bin. For inclusive jets, the boxes around the points indicate combined statistical and systematic uncertainties, although they are dominated by the latter. The bands of the theoretical calculations represent ranges of model parameters (see text). The vertical bars associated with the CoLBT calculation indicate the statistical uncertainties. The shaded bars on the left of the axis at $R_{\mathrm{AA}} = 1$ indicate the p_{T}-independent uncertainties associated with the luminosity in pp collisions and $\langle T_{\mathrm{AA}} \rangle$ for 0–10% Pb+Pb collisions, respectively.

ratio systematically decreases with increasing $p_{\mathrm{T}}^{\mathrm{jet}}$, as the quark-initiated fraction in the two samples become more similar, which is also qualitatively present in the data. However, the agreement with the models is worse, with only the CoLBT model describing the measured double ratio. Since these models otherwise described the inclusive jet R_{AA} well, this additional comparison highlights the need to test them against multiple observables simultaneously to evaluate the description of the colour-charge dependence of energy loss.

9 Conclusion

This Letter presents a measurement of photon-tagged jet production in 1.7 nb^{-1} of Pb+Pb and 260 pb^{-1} of pp collisions at $\sqrt{s_{\mathrm{NN}}} = 5.02$ TeV with the ATLAS detector. The cross-section of jets produced opposite in azimuth ($\Delta\phi > 7\pi/8$) to a $p_{\mathrm{T}}^{\gamma} > 50$ GeV isolated photon is reported as a function of $p_{\mathrm{T}}^{\mathrm{jet}}$. This selection results in a sample of jets with a steeply falling p_{T} distribution and a large fraction of quark-initiated jets. The nuclear modification factor, R_{AA}, for photon-tagged jets is found to be suppressed below unity in a way that varies with centrality but only weakly with $p_{\mathrm{T}}^{\mathrm{jet}}$ in the measured range. The fractional energy loss, S_{loss}, is determined to be approximately 0.10 with no strong p_{T} dependence within uncertainties in the 0–10% centrality interval. The photon-tagged jet R_{AA} (S_{loss}) is significantly higher (lower) than that for inclusive jets at the same $p_{\mathrm{T}}^{\mathrm{jet}}$ and centrality, which instead have a large gluon-initiated jet fraction. The results are compared with a variety of theoretical calculations, which qualitatively describe aspects of the ordering between photon-tagged and inclusive jets, but tend to over-predict the amount of energy loss for the former. The data provide the strongest confirmation to date of larger jet quenching for gluon jets compared with quark jets.

Acknowledgements

We thank CERN for the very successful operation of the LHC, as well as the support staff from our institutions without whom ATLAS could not be operated efficiently.

We acknowledge the support of ANPCyT, Argentina; YerPhI, Armenia; ARC, Australia; BMWFW and FWF, Austria; ANAS, Azerbaijan; CNPq and FAPESP, Brazil; NSERC, NRC and CFI, Canada; CERN; ANID, Chile; CAS, MOST and NSFC, China; Minciencias, Colombia; MEYS CR, Czech Republic; DNRF and DNSRC, Denmark; IN2P3-CNRS and CEA-DRF/IRFU, France; SRNSFG, Georgia; BMBF, HGF and MPG, Germany; GSRI, Greece; RGC and Hong Kong SAR, China; ISF and Benoziyo Center, Israel; INFN, Italy; MEXT and JSPS, Japan; CNRST, Morocco; NWO, Netherlands; RCN, Norway; MEiN, Poland; FCT, Portugal; MNE/IFA, Romania; MESTD, Serbia; MSSR, Slovakia; ARRS and MIZŠ, Slovenia; DSI/NRF, South Africa; MICINN, Spain; SRC and Wallenberg Foundation, Sweden; SERI, SNSF and Cantons of Bern and Geneva, Switzerland; MOST, Taiwan; TENMAK, Türkiye; STFC, United Kingdom; DOE and NSF, United States of America. In addition, individual groups and members have received support from BCKDF, CANARIE, Compute Canada and CRC, Canada; PRIMUS 21/SCI/017 and UNCE SCI/013, Czech Republic; COST, ERC, ERDF, Horizon 2020 and Marie Skłodowska-Curie Actions, European Union; Investissements d'Avenir Labex, Investissements d'Avenir Idex and ANR, France; DFG and AvH Foundation, Germany; Herakleitos, Thales and Aristeia programmes co-financed by EU-ESF and the Greek NSRF, Greece; BSF-NSF and MINERVA, Israel; Norwegian Financial Mechanism 2014-2021, Norway; NCN and NAWA, Poland; La Caixa Banking Foundation, CERCA Programme Generalitat de Catalunya and PROMETEO and GenT Programmes Generalitat Valenciana, Spain; Göran Gustafssons Stiftelse, Sweden; The Royal Society and Leverhulme Trust, United Kingdom.

The crucial computing support from all WLCG partners is acknowledged gratefully, in particular from CERN, the ATLAS Tier-1 facilities at TRIUMF (Canada), NDGF (Denmark, Norway, Sweden), CC-IN2P3 (France), KIT/GridKA (Germany), INFN-CNAF (Italy), NL-T1 (Netherlands), PIC (Spain), ASGC (Taiwan), RAL (UK) and BNL (USA), the Tier-2 facilities worldwide and large non-WLCG resource providers. Major contributors of computing resources are listed in Ref. [79].

References

[1] P. Romatschke and U. Romatschke, *Relativistic Fluid Dynamics In and Out of Equilibrium*, Cambridge Monographs on Mathematical Physics, Cambridge University Press, 2019, ISBN: 978-1-108-48368-1, 978-1-108-75002-8, arXiv: 1712.05815 [nucl-th].

[2] U. Heinz and R. Snellings, *Collective flow and viscosity in relativistic heavy-ion collisions*, Ann. Rev. Nucl. Part. Sci. **63** (2013) 123, arXiv: 1301.2826 [nucl-th].

[3] H. Elfner and B. Müller, *The exploration of hot and dense nuclear matter: Introduction to relativistic heavy-ion physics*, (2022), arXiv: 2210.12056 [nucl-th].

[4] L. Cunqueiro and A. M. Sickles, *Studying the QGP with Jets at the LHC and RHIC*, Prog. Part. Nucl. Phys. **124** (2022) 103940, arXiv: 2110.14490 [nucl-ex].

[5] M. L. Miller, K. Reygers, S. J. Sanders and P. Steinberg, *Glauber modeling in high energy nuclear collisions*, Ann. Rev. Nucl. Part. Sci. **57** (2007) 205, arXiv: nucl-ex/0701025.

[6] CMS Collaboration, *Measurement of transverse momentum relative to dijet systems in PbPb and pp collisions at* $\sqrt{s_{NN}} = 2.76$ *TeV*, JHEP **01** (2016) 006, arXiv: 1509.09029 [hep-ex].

[7] ATLAS Collaboration, *Measurement of angular and momentum distributions of charged particles within and around jets in Pb+Pb and pp collisions at* $\sqrt{s_{NN}} = 5.02$ *TeV with the ATLAS detector*, Phys. Rev. C **100** (2019) 064901, arXiv: 1908.05264 [hep-ex], Erratum: Phys. Rev. C **101** (2019) 059903.

[8] ATLAS Collaboration, *Measurement of the nuclear modification factor for inclusive jets in Pb+Pb collisions at* $\sqrt{s_{NN}} = 5.02$ *TeV with the ATLAS detector*, Phys. Lett. B **790** (2019) 108, arXiv: 1805.05635 [hep-ex].

[9] CMS Collaboration, *First measurement of large area jet transverse momentum spectra in heavy-ion collisions*, JHEP **05** (2021) 284, arXiv: 2102.13080 [hep-ex].

[10] ALICE Collaboration, *Measurements of inclusive jet spectra in pp and central Pb-Pb collisions at* $\sqrt{s_{\mathrm{NN}}} = 5.02$ *TeV*, Phys. Rev. C **101** (2020) 034911, arXiv: 1909.09718 [nucl-ex].

[11] K. Kovařík et al., *nCTEQ15 - Global analysis of nuclear parton distributions with uncertainties in the CTEQ framework*, Phys. Rev. D **93** (2016) 085037, arXiv: 1509.00792 [hep-ph].

[12] K. J. Eskola, P. Paakkinen, H. Paukkunen and C. A. Salgado, *EPPS21: a global QCD analysis of nuclear PDFs*, Eur. Phys. J. C **82** (2022) 413, arXiv: 2112.12462 [hep-ph].

[13] R. Abdul Khalek et al., *nNNPDF3.0: evidence for a modified partonic structure in heavy nuclei*, Eur. Phys. J. C **82** (2022) 507, arXiv: 2201.12363 [hep-ph].

[14] M. Spousta and B. Cole, *Interpreting single jet measurements in Pb + Pb collisions at the LHC*, Eur. Phys. J. C **76** (2016) 50, arXiv: 1504.05169 [hep-ph].

[15] Y. Mehtar-Tani, D. Pablos and K. Tywoniuk, *Cone-Size Dependence of Jet Suppression in Heavy-Ion Collisions*, Phys. Rev. Lett. **127** (2021) 252301, arXiv: 2101.01742 [hep-ph].

[16] A. Takacs and K. Tywoniuk, *Quenching effects in the cumulative jet spectrum*, JHEP **10** (2021) 038, arXiv: 2103.14676 [hep-ph].

[17] W. Ke, Y. Xu and S. A. Bass, *Modified Boltzmann approach for modeling the splitting vertices induced by the hot QCD medium in the deep Landau-Pomeranchuk-Migdal region*, Phys. Rev. C **100** (2019) 064911, arXiv: 1810.08177 [nucl-th].

[18] W. Ke, Y. Xu and S. A. Bass, *Linearized Boltzmann-Langevin model for heavy quark transport in hot and dense QCD matter*, Phys. Rev. C **98** (2018) 064901, arXiv: 1806.08848 [nucl-th].

[19] W. Ke and X.-N. Wang, *QGP modification to single inclusive jets in a calibrated transport model*, JHEP **05** (2021) 041, arXiv: 2010.13680 [hep-ph].

[20] Z.-B. Kang, I. Vitev and H. Xing, *Vector-boson-tagged jet production in heavy ion collisions at energies available at the CERN Large Hadron Collider*, Phys. Rev. C **96** (2017) 014912, arXiv: 1702.07276 [hep-ph].

[21] H. T. Li and I. Vitev, *Inclusive heavy flavor jet production with semi-inclusive jet functions: from proton to heavy-ion collisions*, JHEP **07** (2019) 148, arXiv: 1811.07905 [hep-ph].

[22] H. T. Li and I. Vitev, *Jet charge modification in dense QCD matter*, Phys. Rev. D **101** (2020) 076020, arXiv: 1908.06979 [hep-ph].

[23] Y. He et al., *Interplaying mechanisms behind single inclusive jet suppression in heavy-ion collisions*, Phys. Rev. C **99** (2019) 054911, arXiv: 1809.02525 [nucl-th].

[24] J. Brewer, J. Thaler and A. P. Turner, *Data-driven quark and gluon jet modification in heavy-ion collisions*, Phys. Rev. C **103** (2021) L021901, arXiv: 2008.08596 [hep-ph].

[25] J. Brewer, Q. Brodsky and K. Rajagopal, *Disentangling jet modification in jet simulations and in Z+jet data*, JHEP **02** (2022) 175, arXiv: 2110.13159 [hep-ph].

[26] ATLAS Collaboration, *Measurement of the nuclear modification factor of b-jets in* 5.02 *TeV Pb+Pb collisions with the ATLAS detector*, (2022), arXiv: 2204.13530 [nucl-ex].

[27] CMS Collaboration, *Evidence of b-Jet Quenching in PbPb Collisions at* $\sqrt{s_{NN}} = 2.76$ *TeV*, Phys. Rev. Lett. **113** (2014) 132301, arXiv: 1312.4198 [hep-ex].

[28] ATLAS Collaboration, *Centrality, rapidity and transverse momentum dependence of isolated prompt photon production in lead–lead collisions at* $\sqrt{s_{NN}} = 2.76$ *TeV measured with the ATLAS detector*, Phys. Rev. C **93** (2016) 034914, arXiv: 1506.08552 [hep-ex].

[29] CMS Collaboration, *The production of isolated photons in PbPb and pp collisions at* $\sqrt{s_{NN}} = 5.02$ *TeV*, JHEP **07** (2020) 116, arXiv: 2003.12797 [hep-ex].

[30] ATLAS Collaboration, *Measurement of* $W^{\pm}$ *boson production in Pb+Pb collisions at* $\sqrt{s_{NN}} = 5.02$ *TeV with the ATLAS detector*, Eur. Phys. J. C **79** (2019) 935, arXiv: 1907.10414 [hep-ex].

[31] CMS Collaboration, *Using Z boson events to study parton–medium interactions in PbPb collisions*, Phys. Rev. Lett. **128** (2021) 122301, arXiv: 2103.04377 [hep-ex].

[32] X.-N. Wang, Z. Huang and I. Sarcevic, *Jet quenching in the opposite direction of a tagged photon in high-energy heavy ion collisions*, Phys. Rev. Lett. **77** (1996) 231, arXiv: hep-ph/9605213.

[33] ATLAS Collaboration, *Measurement of photon-jet transverse momentum correlations in* 5.02 *TeV Pb+Pb and pp collisions with ATLAS*, Phys. Lett. B **789** (2019) 167, arXiv: 1809.07280 [hep-ex].

[34] ATLAS Collaboration, *Medium-Induced Modification of Z-Tagged Charged Particle Yields in Pb+Pb Collisions at* 5.02 *TeV with the ATLAS Detector*, Phys. Rev. Lett. **126** (2021) 072301, arXiv: 2008.09811 [hep-ex].

[35] ATLAS Collaboration, *Comparison of Fragmentation Functions for Jets Dominated by Light Quarks and Gluons from pp and Pb+Pb Collisions in ATLAS*, Phys. Rev. Lett. **123** (2019) 042001, arXiv: 1902.10007 [hep-ex].

[36] PHENIX Collaboration, *Formation of dense partonic matter in relativistic nucleus-nucleus collisions at RHIC: Experimental evaluation by the PHENIX collaboration*, Nucl. Phys. A **757** (2005) 184, arXiv: nucl-ex/0410003.

[37] PHENIX Collaboration, *Detailed study of high-p_T neutral pion suppression and azimuthal anisotropy in Au+Au Collisions at $\sqrt{s_{NN}}$ = 200 GeV*, Phys. Rev. C **76** (2007) 034904, arXiv: nucl-ex/0611007.

[38] PHENIX Collaboration, *Scaling properties of fractional momentum loss of high-p_T hadrons in nucleus-nucleus collisions at $\sqrt{s_{NN}}$ from 62.4 GeV to 2.76 TeV*, Phys. Rev. C **93** (2016) 024911, arXiv: 1509.06735 [nucl-ex].

[39] J. Brewer, J. G. Milhano and J. Thaler, *Sorting out quenched jets*, Phys. Rev. Lett. **122** (2019) 222301, arXiv: 1812.05111 [hep-ph].

[40] ATLAS Collaboration, *The ATLAS Experiment at the CERN Large Hadron Collider*, JINST **3** (2008) S08003.

[41] ATLAS Collaboration, *Performance of the ATLAS trigger system in 2015*, Eur. Phys. J. C **77** (2017) 317, arXiv: 1611.09661 [hep-ex].

[42] ATLAS Collaboration, *The ATLAS Collaboration Software and Firmware*, ATL-SOFT-PUB-2021-001, 2021, URL: https://cds.cern.ch/record/2767187.

[43] ATLAS Collaboration, *Performance of electron and photon triggers in ATLAS during LHC Run 2*, Eur. Phys. J. C **80** (2020) 47, arXiv: 1909.00761 [hep-ex].

[44] ATLAS Collaboration, *Prompt and non-prompt J/ψ and $\psi(2S)$ suppression at high transverse momentum in 5.02 TeV Pb+Pb collisions with the ATLAS experiment*, Eur. Phys. J. C **78** (2018) 762, arXiv: 1805.04077 [hep-ex].

[45] ATLAS Collaboration, *Electron and photon performance measurements with the ATLAS detector using the 2015–2017 LHC proton–proton collision data*, JINST **14** (2019) P12006, arXiv: 1908.00005 [hep-ex].

[46] ATLAS Collaboration, *Measurement of the jet radius and transverse momentum dependence of inclusive jet suppression in lead–lead collisions at $\sqrt{s_{NN}}$ = 2.76 TeV with the ATLAS detector*, Phys. Lett. B **719** (2013) 220, arXiv: 1208.1967 [hep-ex].

[47] ATLAS Collaboration, *Measurement of the photon identification efficiencies with the ATLAS detector using LHC Run 2 data collected in 2015 and 2016*, Eur. Phys. J. C **79** (2019) 205, arXiv: 1810.05087 [hep-ex].

[48] M. Cacciari, G. P. Salam and G. Soyez, *The anti-k_t jet clustering algorithm*, JHEP **04** (2008) 063, arXiv: 0802.1189 [hep-ph].

[49] M. Cacciari, G. P. Salam and G. Soyez, *FastJet User Manual*, Eur. Phys. J. C **72** (2012) 1896, arXiv: 1111.6097 [hep-ph].

[50] ATLAS Collaboration, *Jet energy measurement and its systematic uncertainty in proton–proton collisions at $\sqrt{s}$ = 7 TeV with the ATLAS detector*, Eur. Phys. J. C **75** (2015) 17, arXiv: 1406.0076 [hep-ex].

[51] ATLAS Collaboration, *Jet energy scale measurements and their systematic uncertainties in proton–proton collisions at $\sqrt{s}$ = 13 TeV with the ATLAS detector*, Phys. Rev. D **96** (2017) 072002, arXiv: 1703.09665 [hep-ex].

[52] ATLAS Collaboration, *Jet energy scale and its uncertainty for jets reconstructed using the ATLAS heavy ion jet algorithm*, ATLAS-CONF-2015-016, 2015, URL: https://cds.cern.ch/record/2008677.

[53] T. Sjostrand, S. Mrenna and P. Z. Skands, *A brief introduction to PYTHIA 8.1*, Comput. Phys. Commun. **178** (2008) 852, arXiv: 0710.3820 [hep-ph].

[54] ATLAS Collaboration, *ATLAS Pythia 8 tunes to 7 TeV data*, ATL-PHYS-PUB-2014-021, 2014, URL: https://cds.cern.ch/record/1966419.

[55] R. D. Ball et al., *Parton distributions with LHC data*, Nucl. Phys. B **867** (2013) 244, arXiv: 1207.1303 [hep-ph].

[56] E. Bothmann et al., *Event generation with Sherpa 2.2*, SciPost Phys. **7** (2019) 034, arXiv: 1905.09127 [hep-ph].

[57] F. Siegert, *A practical guide to event generation for prompt photon production with Sherpa*, J. Phys. G **44** (2017) 044007, arXiv: 1611.07226 [hep-ph].

[58] R. D. Ball et al., *Parton distributions for the LHC Run II*, JHEP **04** (2015) 040, arXiv: 1410.8849 [hep-ph].

[59] J. Bellm et al., *Herwig 7.0/Herwig++ 3.0 release note*, Eur. Phys. J. C **76** (2016) 196, arXiv: 1512.01178 [hep-ph].

[60] L. Harland-Lang, A. Martin, P. Motylinski and R. Thorne, *Parton distributions in the LHC era: MMHT 2014 PDFs*, Eur. Phys. J. C **75** (2015) 204, arXiv: 1412.3989 [hep-ph].

[61] S. Agostinelli et al., *GEANT4–a simulation toolkit*, Nucl. Instrum. Meth. A **506** (2003) 250.

[62] ATLAS Collaboration, *Light-quark and gluon jet discrimination in pp collisions at $\sqrt{s} = 7$ TeV with the ATLAS detector*, Eur. Phys. J. C **74** (2014) 3023, arXiv: 1405.6583 [hep-ex].

[63] K. J. Eskola, P. Paakkinen, H. Paukkunen and C. A. Salgado, *EPPS16: Nuclear parton distributions with LHC data*, Eur. Phys. J. C **77** (2017) 163, arXiv: 1612.05741 [hep-ph].

[64] ATLAS Collaboration, *Dynamics of isolated-photon plus jet production in pp collisions at $\sqrt{s} = 7$ TeV with the ATLAS detector*, Nucl. Phys. B **875** (2013) 483, arXiv: 1307.6795 [hep-ex].

[65] ATLAS Collaboration, *Measurement of the inclusive isolated prompt photon cross section in pp collisions at $\sqrt{s} = 8$ TeV with the ATLAS detector*, JHEP **08** (2016) 005, arXiv: 1605.03495 [hep-ex].

[66] ATLAS Collaboration, *Measurement of the cross section for inclusive isolated-photon production in pp collisions at $\sqrt{s} = 13$ TeV using the ATLAS detector*, Phys. Lett. B **770** (2017) 473, arXiv: 1701.06882 [hep-ex].

[67] ATLAS Collaboration, *Measurement of the inclusive isolated prompt photons cross section in pp collisions at $\sqrt{s} = 7$ TeV with the ATLAS detector using $4.6\,fb^{-1}$*, Phys. Rev. D **89** (2014) 052004, arXiv: 1311.1440 [hep-ex].

[68] ATLAS Collaboration, *High-E_T isolated-photon plus jets production in pp collisions at $\sqrt{s} = 8$ TeV with the ATLAS detector*, Nucl. Phys. B **918** (2017) 257, arXiv: 1611.06586 [hep-ex].

[69] G. D'Agostini, *A Multidimensional unfolding method based on Bayes' theorem*, Nucl. Instrum. Meth. A **362** (1995) 487.

[70] T. Adye, *Unfolding algorithms and tests using RooUnfold*, Proceedings, PHYSTAT 2011 Workshop on Statistical Issues Related to Discovery Claims in Search Experiments and Unfolding, CERN, Geneva, Switzerland 17-20 January 2011 (2011) p. 313, arXiv: 1105.1160 [physics.data-an].

[71] ATLAS Collaboration, *Electron and photon energy calibration with the ATLAS detector using 2015–2016 LHC proton–proton collision data*, JINST **14** (2019) P03017, arXiv: 1812.03848 [hep-ex].

[72] ATLAS Collaboration, *Measurements of azimuthal anisotropies of jet production in Pb+Pb collisions at* $\sqrt{s_{NN}} = 5.02$ *TeV with the ATLAS detector*, Phys. Rev. C **105** (2021) 064903, arXiv: 2111.06606 [nucl-ex].

[73] ATLAS Collaboration, *Jet energy measurement with the ATLAS detector in proton–proton collisions at* $\sqrt{s} = 7$ *TeV*, Eur. Phys. J. C **73** (2013) 2304, arXiv: 1112.6426 [hep-ex].

[74] ATLAS Collaboration, *Jet energy resolution in proton–proton collisions at* $\sqrt{s} = 7$ *TeV recorded in 2010 with the ATLAS detector*, Eur. Phys. J. C **73** (2013) 2306, arXiv: 1210.6210 [hep-ex].

[75] ATLAS Collaboration, *Determination of jet calibration and energy resolution in proton–proton collisions at* $\sqrt{s} = 8$ *TeV using the ATLAS detector*, Eur. Phys. J. C **80** (2020) 1104, arXiv: 1910.04482 [hep-ex].

[76] ATLAS Collaboration, *Luminosity determination in* pp *collisions at* $\sqrt{s} = 13$ *TeV using the ATLAS detector at the LHC*, (2022), arXiv: 2212.09379 [hep-ex].

[77] ATLAS Collaboration, *Measurement of prompt photon production in* $\sqrt{s_{NN}} = 8.16$ *TeV p+Pb collisions with ATLAS*, Phys. Lett. B **796** (2019) 230, arXiv: 1903.02209 [hep-ex].

[78] R. Kunnawalkam Elayavalli and K. C. Zapp, *Simulating V+jet processes in heavy ion collisions with JEWEL*, Eur. Phys. J. C **76** (2016) 695, arXiv: 1608.03099 [hep-ph].

[79] ATLAS Collaboration, *ATLAS Computing Acknowledgements*, ATL-SOFT-PUB-2021-003, 2021, URL: https://cds.cern.ch/record/2776662.

The ATLAS Collaboration

G. Aad [102], B. Abbott [120], K. Abeling [55], N.J. Abicht [49], S.H. Abidi [29], A. Aboulhorma [35e], H. Abramowicz [151], H. Abreu [150], Y. Abulaiti [117], A.C. Abusleme Hoffman [137a], B.S. Acharya [69a,69b,n], C. Adam Bourdarios [4], L. Adamczyk [85a], L. Adamek [155], S.V. Addepalli [26], J. Adelman [115], A. Adiguzel [21c], T. Adye [134], A.A. Affolder [136], Y. Afik [36], M.N. Agaras [13], J. Agarwala [73a,73b], A. Aggarwal [100], C. Agheorghiesei [27c], A. Ahmad [36], F. Ahmadov [38,y], W.S. Ahmed [104], S. Ahuja [95], X. Ai [62a], G. Aielli [76a,76b], M. Ait Tamlihat [35e], B. Aitbenchikh [35a], I. Aizenberg [168], M. Akbiyik [100], T.P.A. Åkesson [98], A.V. Akimov [37], D. Akiyama [167], N.N. Akolkar [24], K. Al Khoury [41], G.L. Alberghi [23b], J. Albert [164], P. Albicocco [53], G.L. Albouy [60], S. Alderweireldt [52], M. Aleksa [36], I.N. Aleksandrov [38], C. Alexa [27b], T. Alexopoulos [10], A. Alfonsi [114], F. Alfonsi [23b], M. Algren [56], M. Alhroob [120], B. Ali [132], H.M.J. Ali [91], S. Ali [148], S.W. Alibocus [92], M. Aliev [37], G. Alimonti [71a], W. Alkakhi [55], C. Allaire [66], B.M.M. Allbrooke [146], J.F. Allen [52], C.A. Allendes Flores [137f], P.P. Allport [20], A. Aloisio [72a,72b], F. Alonso [90], C. Alpigiani [138], M. Alvarez Estevez [99], A. Alvarez Fernandez [100], M.G. Alviggi [72a,72b], M. Aly [101], Y. Amaral Coutinho [82b], A. Ambler [104], C. Amelung [36], M. Amerl [101], C.G. Ames [109], D. Amidei [106], S.P. Amor Dos Santos [130a], K.R. Amos [162], V. Ananiev [125], C. Anastopoulos [139], T. Andeen [11], J.K. Anders [36], S.Y. Andrean [47a,47b], A. Andreazza [71a,71b], S. Angelidakis [9], A. Angerami [41,ab], A.V. Anisenkov [37], A. Annovi [74a], C. Antel [56], M.T. Anthony [139], E. Antipov [145], M. Antonelli [53], D.J.A. Antrim [17a], F. Anulli [75a], M. Aoki [83], T. Aoki [153], J.A. Aparisi Pozo [162], M.A. Aparo [146], L. Aperio Bella [48], C. Appelt [18], N. Aranzabal [36], C. Arcangeletti [53], A.T.H. Arce [51], E. Arena [92], J-F. Arguin [108], S. Argyropoulos [54], J.-H. Arling [48], A.J. Armbruster [36], O. Arnaez [4], H. Arnold [114], Z.P. Arrubarrena Tame [109], G. Artoni [75a,75b], H. Asada [111], K. Asai [118], S. Asai [153], N.A. Asbah [61], J. Assahsah [35d], K. Assamagan [29], R. Astalos [28a], S. Atashi [159], R.J. Atkin [33a], M. Atkinson [161], N.B. Atlay [18], H. Atmani [62b], P.A. Atmasiddha [106], K. Augsten [132], S. Auricchio [72a,72b], A.D. Auriol [20], V.A. Austrup [101], G. Avolio [36], K. Axiotis [56], G. Azuelos [108,ad], D. Babal [28b], H. Bachacou [135], K. Bachas [152,q], A. Bachiu [34], F. Backman [47a,47b], A. Badea [61], P. Bagnaia [75a,75b], M. Bahmani [18], A.J. Bailey [162], V.R. Bailey [161], J.T. Baines [134], C. Bakalis [10], O.K. Baker [171], E. Bakos [15], D. Bakshi Gupta [8], R. Balasubramanian [114], E.M. Baldin [37], P. Balek [85a], E. Ballabene [23b,23a], F. Balli [135], L.M. Baltes [63a], W.K. Balunas [32], J. Balz [100], E. Banas [86], M. Bandieramonte [129], A. Bandyopadhyay [24], S. Bansal [24], L. Barak [151], M. Barakat [48], E.L. Barberio [105], D. Barberis [57b,57a], M. Barbero [102], G. Barbour [96], K.N. Barends [33a], T. Barillari [110], M-S. Barisits [36], T. Barklow [143], P. Baron [122], D.A. Baron Moreno [101], A. Baroncelli [62a], G. Barone [29], A.J. Barr [126], J.D. Barr [96], L. Barranco Navarro [47a,47b], F. Barreiro [99], J. Barreiro Guimarães da Costa [14a], U. Barron [151], M.G. Barros Teixeira [130a], S. Barsov [37], F. Bartels [63a], R. Bartoldus [143], A.E. Barton [91], P. Bartos [28a], A. Basan [100], M. Baselga [49], A. Bassalat [66], M.J. Basso [155], C.R. Basson [101], R.L. Bates [59], S. Batlamous [35e], J.R. Batley [32], B. Batool [141], M. Battaglia [136], D. Battulga [18], M. Bauce [75a,75b], M. Bauer [36], P. Bauer [24], L.T. Bazzano Hurrell [30], J.B. Beacham [51], T. Beau [127], P.H. Beauchemin [158], F. Becherer [54], P. Bechtle [24], H.P. Beck [19,p], K. Becker [166], A.J. Beddall [21d], V.A. Bednyakov [38], C.P. Bee [145], L.J. Beemster [15], T.A. Beermann [36], M. Begalli [82d,82d], M. Begel [29], A. Behera [145], J.K. Behr [48], J.F. Beirer [55], F. Beisiegel [24], M. Belfkir [116b], G. Bella [151], L. Bellagamba [23b], A. Bellerive [34], P. Bellos [20], K. Beloborodov [37], N.L. Belyaev [37], D. Benchekroun [35a], F. Bendebba [35a], Y. Benhammou [151], M. Benoit [29], J.R. Bensinger [26], S. Bentvelsen [114], L. Beresford [48],

M. Beretta[53], E. Bergeaas Kuutmann[160], N. Berger[4], B. Bergmann[132], J. Beringer[17a], G. Bernardi[5], C. Bernius[143], F.U. Bernlochner[24], F. Bernon[36,102], T. Berry[95], P. Berta[133], A. Berthold[50], I.A. Bertram[91], S. Bethke[110], A. Betti[75a,75b], A.J. Bevan[94], M. Bhamjee[33c], S. Bhatta[145], D.S. Bhattacharya[165], P. Bhattarai[26], V.S. Bhopatkar[121], R. Bi[29,af], R.M. Bianchi[129], G. Bianco[23b,23a], O. Biebel[109], R. Bielski[123], M. Biglietti[77a], T.R.V. Billoud[132], M. Bindi[55], A. Bingul[21b], C. Bini[75a,75b], A. Biondini[92], C.J. Birch-sykes[101], G.A. Bird[20,134], M. Birman[168], M. Biros[133], T. Bisanz[49], E. Bisceglie[43b,43a], D. Biswas[141], A. Bitadze[101], K. Bjørke[125], I. Bloch[48], C. Blocker[26], A. Blue[59], U. Blumenschein[94], J. Blumenthal[100], G.J. Bobbink[114], V.S. Bobrovnikov[37], M. Boehler[54], B. Boehm[165], D. Bogavac[36], A.G. Bogdanchikov[37], C. Bohm[47a], V. Boisvert[95], P. Bokan[48], T. Bold[85a], M. Bomben[5], M. Bona[94], M. Boonekamp[135], C.D. Booth[95], A.G. Borbély[59], I.S. Bordulev[37], H.M. Borecka-Bielska[108], L.S. Borgna[96], G. Borissov[91], D. Bortoletto[126], D. Boscherini[23b], M. Bosman[13], J.D. Bossio Sola[36], K. Bouaouda[35a], N. Bouchhar[162], J. Boudreau[129], E.V. Bouhova-Thacker[91], D. Boumediene[40], R. Bouquet[5], A. Boveia[119], J. Boyd[36], D. Boye[29], I.R. Boyko[38], J. Bracinik[20], N. Brahimi[62d], G. Brandt[170], O. Brandt[32], F. Braren[48], B. Brau[103], J.E. Brau[123], R. Brener[168], L. Brenner[114], R. Brenner[160], S. Bressler[168], D. Britton[59], D. Britzger[110], I. Brock[24], G. Brooijmans[41], W.K. Brooks[137f], E. Brost[29], L.M. Brown[164,l], L.E. Bruce[61], T.L. Bruckler[126], P.A. Bruckman de Renstrom[86], B. Brüers[48], D. Bruncko[28b,*], A. Bruni[23b], G. Bruni[23b], M. Bruschi[23b], N. Bruscino[75a,75b], T. Buanes[16], Q. Buat[138], D. Buchin[110], A.G. Buckley[59], M.K. Bugge[125], O. Bulekov[37], B.A. Bullard[143], S. Burdin[92], C.D. Burgard[49], A.M. Burger[40], B. Burghgrave[8], O. Burlayenko[54], J.T.P. Burr[32], C.D. Burton[11], J.C. Burzynski[142], E.L. Busch[41], V. Büscher[100], P.J. Bussey[59], J.M. Butler[25], C.M. Buttar[59], J.M. Butterworth[96], W. Buttinger[134], C.J. Buxo Vazquez[107], A.R. Buzykaev[37], G. Cabras[23b], S. Cabrera Urbán[162], D. Caforio[58], H. Cai[129], Y. Cai[14a,14e], V.M.M. Cairo[36], O. Cakir[3a], N. Calace[36], P. Calafiura[17a], G. Calderini[127], P. Calfayan[68], G. Callea[59], L.P. Caloba[82b], D. Calvet[40], S. Calvet[40], T.P. Calvet[102], M. Calvetti[74a,74b], R. Camacho Toro[127], S. Camarda[36], D. Camarero Munoz[26], P. Camarri[76a,76b], M.T. Camerlingo[72a,72b], D. Cameron[125], C. Camincher[164], M. Campanelli[96], A. Camplani[42], V. Canale[72a,72b], A. Canesse[104], M. Cano Bret[80], J. Cantero[162], Y. Cao[161], F. Capocasa[26], M. Capua[43b,43a], A. Carbone[71a,71b], R. Cardarelli[76a], J.C.J. Cardenas[8], F. Cardillo[162], T. Carli[36], G. Carlino[72a], J.I. Carlotto[13], B.T. Carlson[129,r], E.M. Carlson[164,156a], L. Carminati[71a,71b], A. Carnelli[135], M. Carnesale[75a,75b], S. Caron[113], E. Carquin[137f], S. Carrá[71a,71b], G. Carratta[23b,23a], F. Carrio Argos[33g], J.W.S. Carter[155], T.M. Carter[52], M.P. Casado[13,i], M. Caspar[48], E.G. Castiglia[171], F.L. Castillo[4], L. Castillo Garcia[13], V. Castillo Gimenez[162], N.F. Castro[130a,130e], A. Catinaccio[36], J.R. Catmore[125], V. Cavaliere[29], N. Cavalli[23b,23a], V. Cavasinni[74a,74b], Y.C. Cekmecelioglu[48], E. Celebi[21a], F. Celli[126], M.S. Centonze[70a,70b], K. Cerny[122], A.S. Cerqueira[82a], A. Cerri[146], L. Cerrito[76a,76b], F. Cerutti[17a], B. Cervato[141], A. Cervelli[23b], G. Cesarini[53], S.A. Cetin[21d], Z. Chadi[35a], D. Chakraborty[115], M. Chala[130f], J. Chan[169], W.Y. Chan[153], J.D. Chapman[32], E. Chapon[135], B. Chargeishvili[149b], D.G. Charlton[20], T.P. Charman[94], M. Chatterjee[19], C. Chauhan[133], S. Chekanov[6], S.V. Chekulaev[156a], G.A. Chelkov[38,a], A. Chen[106], B. Chen[151], B. Chen[164], H. Chen[14c], H. Chen[29], J. Chen[62c], J. Chen[142], M. Chen[126], S. Chen[153], S.J. Chen[14c], X. Chen[62c], X. Chen[14b,ac], Y. Chen[62a], C.L. Cheng[169], H.C. Cheng[64a], S. Cheong[143], A. Cheplakov[38], E. Cheremushkina[48], E. Cherepanova[114], R. Cherkaoui El Moursli[35e], E. Cheu[7], K. Cheung[65], L. Chevalier[135], V. Chiarella[53], G. Chiarelli[74a], N. Chiedde[102], G. Chiodini[70a], A.S. Chisholm[20], A. Chitan[27b],

M. Chitishvili [162], M.V. Chizhov [38], K. Choi [11], A.R. Chomont [75a,75b], Y. Chou [103], E.Y.S. Chow [114], T. Chowdhury [33g], K.L. Chu[168], M.C. Chu [64a], X. Chu [14a,14e], J. Chudoba [131], J.J. Chwastowski [86], D. Cieri [110], K.M. Ciesla [85a], V. Cindro [93], A. Ciocio [17a], F. Cirotto [72a,72b], Z.H. Citron [168], M. Citterio [71a], D.A. Ciubotaru[27b], B.M. Ciungu [155], A. Clark [56], P.J. Clark [52], J.M. Clavijo Columbie [48], S.E. Clawson [48], C. Clement [47a,47b], J. Clercx [48], L. Clissa [23b,23a], Y. Coadou [102], M. Cobal [69a,69c], A. Coccaro [57b], R.F. Coelho Barrue [130a], R. Coelho Lopes De Sa [103], S. Coelli [71a], H. Cohen [151], A.E.C. Coimbra [71a,71b], B. Cole [41], J. Collot [60], P. Conde Muiño [130a,130g], M.P. Connell [33c], S.H. Connell [33c], I.A. Connelly [59], E.I. Conroy [126], F. Conventi [72a,ae], H.G. Cooke [20], A.M. Cooper-Sarkar [126], A. Cordeiro Oudot Choi [127], F. Cormier [163], L.D. Corpe [40], M. Corradi [75a,75b], F. Corriveau [104,w], A. Cortes-Gonzalez [18], M.J. Costa [162], F. Costanza [4], D. Costanzo [139], B.M. Cote [119], G. Cowan [95], K. Cranmer [169], D. Cremonini [23b,23a], S. Crépé-Renaudin [60], F. Crescioli [127], M. Cristinziani [141], M. Cristoforetti [78a,78b], V. Croft [114], J.E. Crosby [121], G. Crosetti [43b,43a], A. Cueto [99], T. Cuhadar Donszelmann [159], H. Cui [14a,14e], Z. Cui [7], W.R. Cunningham [59], F. Curcio [43b,43a], P. Czodrowski [36], M.M. Czurylo [63b], M.J. Da Cunha Sargedas De Sousa [62a], J.V. Da Fonseca Pinto [82b], C. Da Via [101], W. Dabrowski [85a], T. Dado [49], S. Dahbi [33g], T. Dai [106], C. Dallapiccola [103], M. Dam [42], G. D'amen [29], V. D'Amico [109], J. Damp [100], J.R. Dandoy [128], M.F. Daneri [30], M. Danninger [142], V. Dao [36], G. Darbo [57b], S. Darmora [6], S.J. Das [29], S. D'Auria [71a,71b], C. David [156b], T. Davidek [133], B. Davis-Purcell [34], I. Dawson [94], H.A. Day-hall [132], K. De [8], R. De Asmundis [72a], N. De Biase [48], S. De Castro [23b,23a], N. De Groot [113], P. de Jong [114], H. De la Torre [107], A. De Maria [14c], A. De Salvo [75a], U. De Sanctis [76a,76b], A. De Santo [146], J.B. De Vivie De Regie [60], D.V. Dedovich[38], J. Degens [114], A.M. Deiana [44], F. Del Corso [23b,23a], J. Del Peso [99], F. Del Rio [63a], F. Deliot [135], C.M. Delitzsch [49], M. Della Pietra [72a,72b], D. Della Volpe [56], A. Dell'Acqua [36], L. Dell'Asta [71a,71b], M. Delmastro [4], P.A. Delsart [60], S. Demers [171], M. Demichev [38], S.P. Denisov [37], L. D'Eramo [40], D. Derendarz [86], F. Derue [127], P. Dervan [92], K. Desch [24], C. Deutsch [24], F.A. Di Bello [57b,57a], A. Di Ciaccio [76a,76b], L. Di Ciaccio [4], A. Di Domenico [75a,75b], C. Di Donato [72a,72b], A. Di Girolamo [36], G. Di Gregorio [5], A. Di Luca [78a,78b], B. Di Micco [77a,77b], R. Di Nardo [77a,77b], C. Diaconu [102], F.A. Dias [114], T. Dias Do Vale [142], M.A. Diaz [137a,137b], F.G. Diaz Capriles [24], M. Didenko [162], E.B. Diehl [106], L. Diehl [54], S. Díez Cornell [48], C. Diez Pardos [141], C. Dimitriadi [24,160], A. Dimitrievska [17a], J. Dingfelder [24], I-M. Dinu [27b], S.J. Dittmeier [63b], F. Dittus [36], F. Djama [102], T. Djobava [149b], J.I. Djuvsland [16], C. Doglioni [101,98], J. Dolejsi [133], Z. Dolezal [133], M. Donadelli [82c], B. Dong [107], J. Donini [40], A. D'Onofrio [77a,77b], M. D'Onofrio [92], J. Dopke [134], A. Doria [72a], N. Dos Santos Fernandes [130a], M.T. Dova [90], A.T. Doyle [59], M.A. Draguet [126], E. Dreyer [168], I. Drivas-koulouris [10], A.S. Drobac [158], M. Drozdova [56], D. Du [62a], T.A. du Pree [114], F. Dubinin [37], M. Dubovsky [28a], E. Duchovni [168], G. Duckeck [109], O.A. Ducu [27b], D. Duda [52], A. Dudarev [36], E.R. Duden [26], M. D'uffizi [101], L. Duflot [66], M. Dührssen [36], C. Dülsen [170], A.E. Dumitriu [27b], M. Dunford [63a], S. Dungs [49], K. Dunne [47a,47b], A. Duperrin [102], H. Duran Yildiz [3a], M. Düren [58], A. Durglishvili [149b], B.L. Dwyer [115], G.I. Dyckes [17a], M. Dyndal [85a], S. Dysch [101], B.S. Dziedzic [86], Z.O. Earnshaw [146], G.H. Eberwein [126], B. Eckerova [28a], S. Eggebrecht [55], M.G. Eggleston[51], E. Egidio Purcino De Souza [127], L.F. Ehrke [56], G. Eigen [16], K. Einsweiler [17a], T. Ekelof [160], P.A. Ekman [98], Y. El Ghazali [35b], H. El Jarrari [35e,148], A. El Moussaouy [35a], V. Ellajosyula [160], M. Ellert [160], F. Ellinghaus [170], A.A. Elliot [94], N. Ellis [36], J. Elmsheuser [29], M. Elsing [36], D. Emeliyanov [134], Y. Enari [153], I. Ene [17a], S. Epari [13], J. Erdmann [49], P.A. Erland [86], M. Errenst [170], M. Escalier [66], C. Escobar [162], E. Etzion [151], G. Evans [130a], H. Evans [68], L.S. Evans [95], M.O. Evans [146],

A. Ezhilov [37], S. Ezzarqtouni [35a], F. Fabbri [59], L. Fabbri [23b,23a], G. Facini [96], V. Fadeyev [136], R.M. Fakhrutdinov [37], S. Falciano [75a], L.F. Falda Ulhoa Coelho [36], P.J. Falke [24], J. Faltova [133], C. Fan [161], Y. Fan [14a], Y. Fang [14a,14e], M. Fanti [71a,71b], M. Faraj [69a,69b], Z. Farazpay[97], A. Farbin [8], A. Farilla [77a], T. Farooque [107], S.M. Farrington [52], F. Fassi [35e], D. Fassouliotis [9], M. Faucci Giannelli [76a,76b], W.J. Fawcett [32], L. Fayard [66], P. Federic [133], P. Federicova [131], O.L. Fedin [37,a], G. Fedotov [37], M. Feickert [169], L. Feligioni [102], A. Fell [139], D.E. Fellers [123], C. Feng [62b], M. Feng [14b], Z. Feng [114], M.J. Fenton [159], A.B. Fenyuk[37], L. Ferencz [48], R.A.M. Ferguson [91], S.I. Fernandez Luengo [137f], J.A. Fernandez Pretel [54], M.J.V. Fernoux [102], J. Ferrando [48], A. Ferrari [160], P. Ferrari [114,113], R. Ferrari [73a], D. Ferrere [56], C. Ferretti [106], F. Fiedler [100], A. Filipčič [93], E.K. Filmer [1], F. Filthaut [113], M.C.N. Fiolhais [130a,130c,c], L. Fiorini [162], W.C. Fisher [107], T. Fitschen [101], P.M. Fitzhugh[135], I. Fleck [141], P. Fleischmann [106], T. Flick [170], L. Flores [128], M. Flores [33d], L.R. Flores Castillo [64a], L. Flores Sanz De Acedo[36], F.M. Follega [78a,78b], N. Fomin [16], J.H. Foo [155], B.C. Forland[68], A. Formica [135], A.C. Forti [101], E. Fortin [36], A.W. Fortman [61], M.G. Foti [17a], L. Fountas [9], D. Fournier [66], H. Fox [91], P. Francavilla [74a,74b], S. Francescato [61], S. Franchellucci [56], M. Franchini [23b,23a], S. Franchino [63a], D. Francis[36], L. Franco [113], L. Franconi [48], M. Franklin [61], G. Frattari [26], A.C. Freegard [94], W.S. Freund [82b], Y.Y. Frid [151], N. Fritzsche [50], A. Froch [54], D. Froidevaux [36], J.A. Frost [126], Y. Fu [62a], M. Fujimoto [118], E. Fullana Torregrosa [162,*], K.Y. Fung [64a], E. Furtado De Simas Filho [82b], M. Furukawa [153], J. Fuster [162], A. Gabrielli [23b,23a], A. Gabrielli [155], P. Gadow [48], G. Gagliardi [57b,57a], L.G. Gagnon [17a], E.J. Gallas [126], B.J. Gallop [134], K.K. Gan [119], S. Ganguly [153], J. Gao [62a], Y. Gao [52], F.M. Garay Walls [137a,137b], B. Garcia[29,af], C. García [162], A. Garcia Alonso [114], A.G. Garcia Caffaro [171], J.E. García Navarro [162], M. Garcia-Sciveres [17a], G.L. Gardner [128], R.W. Gardner [39], N. Garelli [158], D. Garg [80], R.B. Garg [143], J.M. Gargan[52], C.A. Garner[155], S.J. Gasiorowski [138], P. Gaspar [82b], G. Gaudio [73a], V. Gautam[13], P. Gauzzi [75a,75b], I.L. Gavrilenko [37], A. Gavrilyuk [37], C. Gay [163], G. Gaycken [48], E.N. Gazis [10], A.A. Geanta [27b], C.M. Gee [136], C. Gemme [57b], M.H. Genest [60], S. Gentile [75a,75b], S. George [95], W.F. George [20], T. Geralis [46], P. Gessinger-Befurt [36], M.E. Geyik [170], M. Ghneimat [141], K. Ghorbanian [94], A. Ghosal [141], A. Ghosh [159], A. Ghosh [7], B. Giacobbe [23b], S. Giagu [75a,75b], P. Giannetti [74a], A. Giannini [62a], S.M. Gibson [95], M. Gignac [136], D.T. Gil [85b], A.K. Gilbert [85a], B.J. Gilbert [41], D. Gillberg [34], G. Gilles [114], N.E.K. Gillwald [48], L. Ginabat [127], D.M. Gingrich [2,ad], M.P. Giordani [69a,69c], P.F. Giraud [135], G. Giugliarelli [69a,69c], D. Giugni [71a], F. Giuli [36], I. Gkialas [9,j], L.K. Gladilin [37], C. Glasman [99], G.R. Gledhill [123], M. Glisic[123], I. Gnesi [43b,f], Y. Go [29,af], M. Goblirsch-Kolb [36], B. Gocke [49], D. Godin[108], B. Gokturk[21a], S. Goldfarb [105], T. Golling [56], M.G.D. Gololo[33g], D. Golubkov [37], J.P. Gombas [107], A. Gomes [130a,130b], G. Gomes Da Silva [141], A.J. Gomez Delegido [162], R. Gonçalo [130a,130c], G. Gonella [123], L. Gonella [20], A. Gongadze [38], F. Gonnella [20], J.L. Gonski [41], S. González de la Hoz [162], S. Gonzalez Fernandez [13], R. Gonzalez Lopez [92], C. Gonzalez Renteria [17a], R. Gonzalez Suarez [160], S. Gonzalez-Sevilla [56], G.R. Gonzalvo Rodriguez [162], R.Y. González Andana [52], L. Goossens [36], P.A. Gorbounov [37], B. Gorini [36], E. Gorini [70a,70b], A. Gorišek [93], T.C. Gosart [128], A.T. Goshaw [51], M.I. Gostkin [38], S. Goswami [121], C.A. Gottardo [36], M. Gouighri [35b], V. Goumarre [48], A.G. Goussiou [138], N. Govender [33c], I. Grabowska-Bold [85a], K. Graham [34], E. Gramstad [125], S. Grancagnolo [70a,70b], M. Grandi [146], V. Gratchev[37,*], P.M. Gravila [27f], F.G. Gravili [70a,70b], H.M. Gray [17a], M. Greco [70a,70b], C. Grefe [24], I.M. Gregor [48], P. Grenier [143], C. Grieco [13], A.A. Grillo [136], K. Grimm [31], S. Grinstein [13,t], J.-F. Grivaz [66], E. Gross [168], J. Grosse-Knetter [55], C. Grud[106], J.C. Grundy [126], L. Guan [106], W. Guan [169], C. Gubbels [163], J.G.R. Guerrero Rojas [162], G. Guerrieri [69a,69b], F. Guescini [110], R. Gugel [100], J.A.M. Guhit [106], A. Guida [18],

T. Guillemin[4], E. Guilloton[166,134], S. Guindon[36], F. Guo[14a,14e], J. Guo[62c], L. Guo[48], Y. Guo[106], R. Gupta[48], S. Gurbuz[24], S.S. Gurdasani[54], G. Gustavino[36], M. Guth[56], P. Gutierrez[120], L.F. Gutierrez Zagazeta[128], C. Gutschow[96], C. Gwenlan[126], C.B. Gwilliam[92], E.S. Haaland[125], A. Haas[117], M. Habedank[48], C. Haber[17a], H.K. Hadavand[8], A. Hadef[100], S. Hadzic[110], J.J. Hahn[141], E.H. Haines[96], M. Haleem[165], J. Haley[121], J.J. Hall[139], G.D. Hallewell[102], L. Halser[19], K. Hamano[164], H. Hamdaoui[35e], M. Hamer[24], G.N. Hamity[52], E.J. Hampshire[95], J. Han[62b], K. Han[62a], L. Han[14c], L. Han[62a], S. Han[17a], Y.F. Han[155], K. Hanagaki[83], M. Hance[136], D.A. Hangal[41,ab], H. Hanif[142], M.D. Hank[128], R. Hankache[101], J.B. Hansen[42], J.D. Hansen[42], P.H. Hansen[42], K. Hara[157], D. Harada[56], T. Harenberg[170], S. Harkusha[37], Y.T. Harris[126], J. Harrison[13], N.M. Harrison[119], P.F. Harrison[166], N.M. Hartman[143], N.M. Hartmann[109], Y. Hasegawa[140], A. Hasib[52], S. Haug[19], R. Hauser[107], C.M. Hawkes[20], R.J. Hawkings[36], Y. Hayashi[153], S. Hayashida[111], D. Hayden[107], C. Hayes[106], R.L. Hayes[114], C.P. Hays[126], J.M. Hays[94], H.S. Hayward[92], F. He[62a], M. He[14a,14e], Y. He[154], Y. He[127], N.B. Heatley[94], V. Hedberg[98], A.L. Heggelund[125], N.D. Hehir[94], C. Heidegger[54], K.K. Heidegger[54], W.D. Heidorn[81], J. Heilman[34], S. Heim[48], T. Heim[17a], J.G. Heinlein[128], J.J. Heinrich[123], L. Heinrich[110], J. Hejbal[131], L. Helary[48], A. Held[169], S. Hellesund[16], C.M. Helling[163], S. Hellman[47a,47b], C. Helsens[36], R.C.W. Henderson[91], L. Henkelmann[32], A.M. Henriques Correia[36], H. Herde[98], Y. Hernández Jiménez[145], L.M. Herrmann[24], T. Herrmann[50], G. Herten[54], R. Hertenberger[109], L. Hervas[36], M.E. Hesping[100], N.P. Hessey[156a], H. Hibi[84], S.J. Hillier[20], J.R. Hinds[107], F. Hinterkeuser[24], M. Hirose[124], S. Hirose[157], D. Hirschbuehl[170], T.G. Hitchings[101], B. Hiti[93], J. Hobbs[145], R. Hobincu[27e], N. Hod[168], M.C. Hodgkinson[139], B.H. Hodkinson[32], A. Hoecker[36], J. Hofer[48], T. Holm[24], M. Holzbock[110], L.B.A.H. Hommels[32], B.P. Honan[101], J. Hong[62c], T.M. Hong[129], B.H. Hooberman[161], W.H. Hopkins[6], Y. Horii[111], S. Hou[148], A.S. Howard[93], J. Howarth[59], J. Hoya[6], M. Hrabovsky[122], A. Hrynevich[48], T. Hryn'ova[4], P.J. Hsu[65], S.-C. Hsu[138], Q. Hu[41], Y.F. Hu[14a,14e], S. Huang[64b], X. Huang[14c], Y. Huang[62a], Y. Huang[14a], Z. Huang[101], Z. Hubacek[132], M. Huebner[24], F. Huegging[24], T.B. Huffman[126], C.A. Hugli[48], M. Huhtinen[36], S.K. Huiberts[16], R. Hulsken[104], N. Huseynov[12,a], J. Huston[107], J. Huth[61], R. Hyneman[143], G. Iacobucci[56], G. Iakovidis[29], I. Ibragimov[141], L. Iconomidou-Fayard[66], P. Iengo[72a,72b], R. Iguchi[153], T. Iizawa[83,aa], Y. Ikegami[83], N. Ilic[155], H. Imam[35a], M. Ince Lezki[56], T. Ingebretsen Carlson[47a,47b], G. Introzzi[73a,73b], M. Iodice[77a], V. Ippolito[75a,75b], R.K. Irwin[92], M. Ishino[153], W. Islam[169], C. Issever[18,48], S. Istin[21a], H. Ito[167], J.M. Iturbe Ponce[64a], R. Iuppa[78a,78b], A. Ivina[168], J.M. Izen[45], V. Izzo[72a], P. Jacka[131,132], P. Jackson[1], R.M. Jacobs[48], B.P. Jaeger[142], C.S. Jagfeld[109], P. Jain[54], G. Jäkel[170], K. Jakobs[54], T. Jakoubek[168], J. Jamieson[59], K.W. Janas[85a], A.E. Jaspan[92], M. Javurkova[103], F. Jeanneau[135], L. Jeanty[123], J. Jejelava[149a,z], P. Jenni[54,g], C.E. Jessiman[34], S. Jézéquel[4], C. Jia[62b], J. Jia[145], X. Jia[61], X. Jia[14a,14e], Z. Jia[14c], Y. Jiang[62a], S. Jiggins[48], J. Jimenez Pena[13], S. Jin[14c], A. Jinaru[27b], O. Jinnouchi[154], P. Johansson[139], K.A. Johns[7], J.W. Johnson[136], D.M. Jones[32], E. Jones[48], P. Jones[32], R.W.L. Jones[91], T.J. Jones[92], R. Joshi[119], J. Jovicevic[15], X. Ju[17a], J.J. Junggeburth[36], T. Junkermann[63a], A. Juste Rozas[13,t], M.K. Juzek[86], S. Kabana[137e], A. Kaczmarska[86], M. Kado[110], H. Kagan[119], M. Kagan[143], A. Kahn[41], A. Kahn[128], C. Kahra[100], T. Kaji[167], E. Kajomovitz[150], N. Kakati[168], I. Kalaitzidou[54], C.W. Kalderon[29], A. Kamenshchikov[155], S. Kanayama[154], N.J. Kang[136], D. Kar[33g], K. Karava[126], M.J. Kareem[156b], E. Karentzos[54], I. Karkanias[152], O. Karkout[114], S.N. Karpov[38], Z.M. Karpova[38], V. Kartvelishvili[91], A.N. Karyukhin[37], E. Kasimi[152], J. Katzy[48], S. Kaur[34], K. Kawade[140], T. Kawamoto[135], E.F. Kay[36], F.I. Kaya[158], S. Kazakos[107], V.F. Kazanin[37], Y. Ke[145], J.M. Keaveney[33a],

R. Keeler[164], G.V. Kehris[61], J.S. Keller[34], A.S. Kelly[96], J.J. Kempster[146], K.E. Kennedy[41], P.D. Kennedy[100], O. Kepka[131], B.P. Kerridge[166], S. Kersten[170], B.P. Kerševan[93], S. Keshri[66], L. Keszeghova[28a], S. Ketabchi Haghighat[155], M. Khandoga[127], A. Khanov[121], A.G. Kharlamov[37], T. Kharlamova[37], E.E. Khoda[138], T.J. Khoo[18], G. Khoriauli[165], J. Khubua[149b], Y.A.R. Khwaira[66], M. Kiehn[36], A. Kilgallon[123], D.W. Kim[47a,47b], Y.K. Kim[39], N. Kimura[96], A. Kirchhoff[55], C. Kirfel[24], F. Kirfel[24], J. Kirk[134], A.E. Kiryunin[110], C. Kitsaki[10], O. Kivernyk[24], M. Klassen[63a], C. Klein[34], L. Klein[165], M.H. Klein[106], M. Klein[92], S.B. Klein[56], U. Klein[92], P. Klimek[36], A. Klimentov[29], T. Klioutchnikova[36], P. Kluit[114], S. Kluth[110], E. Kneringer[79], T.M. Knight[155], A. Knue[54], R. Kobayashi[87], S.F. Koch[126], M. Kocian[143], P. Kodyš[133], D.M. Koeck[123], P.T. Koenig[24], T. Koffas[34], M. Kolb[135], I. Koletsou[4], T. Komarek[122], K. Köneke[54], A.X.Y. Kong[1], T. Kono[118], N. Konstantinidis[96], B. Konya[98], R. Kopeliansky[68], S. Koperny[85a], K. Korcyl[86], K. Kordas[152,e], G. Koren[151], A. Korn[96], S. Korn[55], I. Korolkov[13], N. Korotkova[37], B. Kortman[114], O. Kortner[110], S. Kortner[110], W.H. Kostecka[115], V.V. Kostyukhin[141], A. Kotsokechagia[135], A. Kotwal[51], A. Koulouris[36], A. Kourkoumeli-Charalampidi[73a,73b], C. Kourkoumelis[9], E. Kourlitis[6], O. Kovanda[146], R. Kowalewski[164], W. Kozanecki[135], A.S. Kozhin[37], V.A. Kramarenko[37], G. Kramberger[93], P. Kramer[100], M.W. Krasny[127], A. Krasznahorkay[36], J.W. Kraus[170], J.A. Kremer[100], T. Kresse[50], J. Kretzschmar[92], K. Kreul[18], P. Krieger[155], S. Krishnamurthy[103], M. Krivos[133], K. Krizka[20], K. Kroeninger[49], H. Kroha[110], J. Kroll[131], J. Kroll[128], K.S. Krowpman[107], U. Kruchonak[38], H. Krüger[24], N. Krumnack[81], M.C. Kruse[51], J.A. Krzysiak[86], O. Kuchinskaia[37], S. Kuday[3a], S. Kuehn[36], R. Kuesters[54], T. Kuhl[48], V. Kukhtin[38], Y. Kulchitsky[37,a], S. Kuleshov[137d,137b], M. Kumar[33g], N. Kumari[102], A. Kupco[131], T. Kupfer[49], A. Kupich[37], O. Kuprash[54], H. Kurashige[84], L.L. Kurchaninov[156a], O. Kurdysh[66], Y.A. Kurochkin[37], A. Kurova[37], M. Kuze[154], A.K. Kvam[103], J. Kvita[122], T. Kwan[104], N.G. Kyriacou[106], L.A.O. Laatu[102], C. Lacasta[162], F. Lacava[75a,75b], H. Lacker[18], D. Lacour[127], N.N. Lad[96], E. Ladygin[38], B. Laforge[127], T. Lagouri[137e], S. Lai[55], I.K. Lakomiec[85a], N. Lalloue[60], J.E. Lambert[164,l], S. Lammers[68], W. Lampl[7], C. Lampoudis[152,e], A.N. Lancaster[115], E. Lançon[29], U. Landgraf[54], M.P.J. Landon[94], V.S. Lang[54], R.J. Langenberg[103], O.K.B. Langrekken[125], A.J. Lankford[159], F. Lanni[36], K. Lantzsch[24], A. Lanza[73a], A. Lapertosa[57b,57a], J.F. Laporte[135], T. Lari[71a], F. Lasagni Manghi[23b], M. Lassnig[36], V. Latonova[131], A. Laudrain[100], A. Laurier[150], S.D. Lawlor[95], Z. Lawrence[101], M. Lazzaroni[71a,71b], B. Le[101], E.M. Le Boulicaut[51], B. Leban[93], A. Lebedev[81], M. LeBlanc[36], F. Ledroit-Guillon[60], A.C.A. Lee[96], S.C. Lee[148], S. Lee[47a,47b], T.F. Lee[92], L.L. Leeuw[33c], H.P. Lefebvre[95], M. Lefebvre[164], C. Leggett[17a], G. Lehmann Miotto[36], M. Leigh[56], W.A. Leight[103], W. Leinonen[113], A. Leisos[152,s], M.A.L. Leite[82c], C.E. Leitgeb[48], R. Leitner[133], K.J.C. Leney[44], T. Lenz[24], S. Leone[74a], C. Leonidopoulos[52], A. Leopold[144], C. Leroy[108], R. Les[107], C.G. Lester[32], M. Levchenko[37], J. Levêque[4], D. Levin[106], L.J. Levinson[168], M.P. Lewicki[86], D.J. Lewis[4], A. Li[5], B. Li[62b], C. Li[62a], C-Q. Li[62c], H. Li[62a], H. Li[62b], H. Li[14c], H. Li[62b], K. Li[138], L. Li[62c], M. Li[14a,14e], Q.Y. Li[62a], S. Li[14a,14e], S. Li[62d,62c,d], T. Li[5,b], X. Li[104], Z. Li[126], Z. Li[104], Z. Li[92], Z. Li[14a,14e], Z. Liang[14a], M. Liberatore[48], B. Liberti[76a], K. Lie[64c], J. Lieber Marin[82b], H. Lien[68], K. Lin[107], R.E. Lindley[7], J.H. Lindon[2], A. Linss[48], E. Lipeles[128], A. Lipniacka[16], A. Lister[163], J.D. Little[4], B. Liu[14a], B.X. Liu[142], D. Liu[62d,62c], J.B. Liu[62a], J.K.K. Liu[32], K. Liu[62d,62c], M. Liu[62a], M.Y. Liu[62a], P. Liu[14a], Q. Liu[62d,138,62c], X. Liu[62a], Y. Liu[14d,14e], Y.L. Liu[106], Y.W. Liu[62a], J. Llorente Merino[142], S.L. Lloyd[94], E.M. Lobodzinska[48], P. Loch[7], S. Loffredo[76a,76b], T. Lohse[18], K. Lohwasser[139], E. Loiacono[48], M. Lokajicek[131], J.D. Lomas[20], J.D. Long[161],

I. Longarini [159], L. Longo [70a,70b], R. Longo [161], I. Lopez Paz [67], A. Lopez Solis [48], J. Lorenz [109], N. Lorenzo Martinez [4], A.M. Lory [109], O. Loseva [37], X. Lou [47a,47b], X. Lou [14a,14e], A. Lounis [66], J. Love [6], P.A. Love [91], G. Lu [14a,14e], M. Lu [80], S. Lu [128], Y.J. Lu [65], H.J. Lubatti [138], C. Luci [75a,75b], F.L. Lucio Alves [14c], A. Lucotte [60], F. Luehring [68], I. Luise [145], O. Lukianchuk [66], O. Lundberg [144], B. Lund-Jensen [144], N.A. Luongo [123], M.S. Lutz [151], D. Lynn [29], H. Lyons[92], R. Lysak [131], E. Lytken [98], V. Lyubushkin [38], T. Lyubushkina [38], M.M. Lyukova [145], H. Ma [29], L.L. Ma [62b], Y. Ma [121], D.M. Mac Donell [164], G. Maccarrone [53], J.C. MacDonald [100], R. Madar [40], W.F. Mader [50], J. Maeda [84], T. Maeno [29], M. Maerker [50], H. Maguire [139], V. Maiboroda [135], A. Maio [130a,130b,130d], K. Maj [85a], O. Majersky [48], S. Majewski [123], N. Makovec [66], V. Maksimovic [15], B. Malaescu [127], Pa. Malecki [86], V.P. Maleev [37], F. Malek [60], M. Mali [93], D. Malito [95,o], U. Mallik [80], S. Maltezos[10], S. Malyukov[38], J. Mamuzic [13], G. Mancini [53], G. Manco [73a,73b], J.P. Mandalia [94], I. Mandić [93], L. Manhaes de Andrade Filho [82a], I.M. Maniatis [168], J. Manjarres Ramos [102], D.C. Mankad [168], A. Mann [109], B. Mansoulie [135], S. Manzoni [36], A. Marantis [152], G. Marchiori [5], M. Marcisovsky [131], C. Marcon [71a,71b], M. Marinescu [20], M. Marjanovic [120], E.J. Marshall [91], Z. Marshall [17a], S. Marti-Garcia [162], T.A. Martin [166], V.J. Martin [52], B. Martin dit Latour [16], L. Martinelli [75a,75b], M. Martinez [13,t], P. Martinez Agullo [162], V.I. Martinez Outschoorn [103], P. Martinez Suarez [13], S. Martin-Haugh [134], V.S. Martoiu [27b], A.C. Martyniuk [96], A. Marzin [36], D. Mascione [78a,78b], L. Masetti [100], T. Mashimo [153], J. Masik [101], A.L. Maslennikov [37], L. Massa [23b], P. Massarotti [72a,72b], P. Mastrandrea [74a,74b], A. Mastroberardino [43b,43a], T. Masubuchi [153], T. Mathisen [160], J. Matousek [133], N. Matsuzawa[153], J. Maurer [27b], B. Maček [93], D.A. Maximov [37], R. Mazini [148], I. Maznas [152], M. Mazza [107], S.M. Mazza [136], E. Mazzeo [71a,71b], C. Mc Ginn [29], J.P. Mc Gowan [104], S.P. Mc Kee [106], E.F. McDonald [105], A.E. McDougall [114], J.A. Mcfayden [146], R.P. McGovern [128], G. Mchedlidze [149b], R.P. Mckenzie [33g], T.C. Mclachlan [48], D.J. Mclaughlin [96], K.D. McLean [164], S.J. McMahon [134], P.C. McNamara [105], C.M. Mcpartland [92], R.A. McPherson [164,w], S. Mehlhase [109], A. Mehta [92], D. Melini [150], B.R. Mellado Garcia [33g], A.H. Melo [55], F. Meloni [48], A.M. Mendes Jacques Da Costa [101], H.Y. Meng [155], L. Meng [91], S. Menke [110], M. Mentink [36], E. Meoni [43b,43a], C. Merlassino [126], L. Merola [72a,72b], C. Meroni [71a], G. Merz[106], O. Meshkov [37], J. Metcalfe [6], A.S. Mete [6], C. Meyer [68], J-P. Meyer [135], R.P. Middleton [134], L. Mijović [52], G. Mikenberg [168], M. Mikestikova [131], M. Mikuž [93], H. Mildner [100], A. Milic [36], C.D. Milke [44], D.W. Miller [39], L.S. Miller [34], A. Milov [168], D.A. Milstead[47a,47b], T. Min[14c], A.A. Minaenko [37], I.A. Minashvili [149b], L. Mince [59], A.I. Mincer [117], B. Mindur [85a], M. Mineev [38], Y. Mino [87], L.M. Mir [13], M. Miralles Lopez [162], M. Mironova [17a], A. Mishima[153], M.C. Missio [113], T. Mitani [167], A. Mitra [166], V.A. Mitsou [162], O. Miu [155], P.S. Miyagawa [94], Y. Miyazaki[89], A. Mizukami [83], T. Mkrtchyan [63a], M. Mlinarevic [96], T. Mlinarevic [96], M. Mlynarikova [36], S. Mobius [19], K. Mochizuki [108], P. Moder [48], P. Mogg [109], A.F. Mohammed [14a,14e], S. Mohapatra [41], G. Mokgatitswane [33g], L. Moleri [168], B. Mondal [141], S. Mondal [132], G. Monig [146], K. Mönig [48], E. Monnier [102], L. Monsonis Romero[162], J. Montejo Berlingen [13,83], M. Montella [119], F. Monticelli [90], S. Monzani [69a,69c], N. Morange [66], A.L. Moreira De Carvalho [130a], M. Moreno Llácer [162], C. Moreno Martinez [56], P. Morettini [57b], S. Morgenstern [36], M. Morii [61], M. Morinaga [153], A.K. Morley [36], F. Morodei [75a,75b], L. Morvaj [36], P. Moschovakos [36], B. Moser [36], M. Mosidze[149b], T. Moskalets [54], P. Moskvitina [113], J. Moss [31,m], E.J.W. Moyse [103], O. Mtintsilana [33g], S. Muanza [102], J. Mueller [129], D. Muenstermann [91], R. Müller [19], G.A. Mullier [160], A.J. Mullin[32], J.J. Mullin[128], D.P. Mungo [155], D. Munoz Perez [162], F.J. Munoz Sanchez [101], M. Murin [101], W.J. Murray [166,134], A. Murrone [71a,71b], J.M. Muse [120], M. Muškinja [17a], C. Mwewa [29], A.G. Myagkov [37,a],

A.J. Myers[8], A.A. Myers[129], G. Myers[68], M. Myska[132], B.P. Nachman[17a], O. Nackenhorst[49], A.Nag Nag[50], K. Nagai[126], K. Nagano[83], J.L. Nagle[29,af], E. Nagy[102], A.M. Nairz[36], Y. Nakahama[83], K. Nakamura[83], K. Nakkalil[5], H. Nanjo[124], R. Narayan[44], E.A. Narayanan[112], I. Naryshkin[37], M. Naseri[34], S. Nasri[116b], C. Nass[24], G. Navarro[22a], J. Navarro-Gonzalez[162], R. Nayak[151], A. Nayaz[18], P.Y. Nechaeva[37], F. Nechansky[48], L. Nedic[126], T.J. Neep[20], A. Negri[73a,73b], M. Negrini[23b], C. Nellist[114], C. Nelson[104], K. Nelson[106], S. Nemecek[131], M. Nessi[36,h], M.S. Neubauer[161], F. Neuhaus[100], J. Neundorf[48], R. Newhouse[163], P.R. Newman[20], C.W. Ng[129], Y.W.Y. Ng[48], B. Ngair[35e], H.D.N. Nguyen[108], R.B. Nickerson[126], R. Nicolaidou[135], J. Nielsen[136], M. Niemeyer[55], J. Niermann[55,36], N. Nikiforou[36], V. Nikolaenko[37,a], I. Nikolic-Audit[127], K. Nikolopoulos[20], P. Nilsson[29], I. Ninca[48], H.R. Nindhito[56], G. Ninio[151], A. Nisati[75a], N. Nishu[2], R. Nisius[110], J-E. Nitschke[50], E.K. Nkadimeng[33g], S.J. Noacco Rosende[90], T. Nobe[153], D.L. Noel[32], T. Nommensen[147], M.B. Norfolk[139], R.R.B. Norisam[96], B.J. Norman[34], J. Novak[93], T. Novak[48], L. Novotny[132], R. Novotny[112], L. Nozka[122], K. Ntekas[159], N.M.J. Nunes De Moura Junior[82b], E. Nurse[96], J. Ocariz[127], A. Ochi[84], I. Ochoa[130a], S. Oerdek[160], J.T. Offermann[39], A. Ogrodnik[133], A. Oh[101], C.C. Ohm[144], H. Oide[83], R. Oishi[153], M.L. Ojeda[48], Y. Okazaki[87], M.W. O'Keefe[92], Y. Okumura[153], L.F. Oleiro Seabra[130a], S.A. Olivares Pino[137d], D. Oliveira Damazio[29], D. Oliveira Goncalves[82a], J.L. Oliver[159], M.J.R. Olsson[159], A. Olszewski[86], Ö.O. Öncel[54], D.C. O'Neil[142], A.P. O'Neill[19], A. Onofre[130a,130e], P.U.E. Onyisi[11], M.J. Oreglia[39], G.E. Orellana[90], D. Orestano[77a,77b], N. Orlando[13], R.S. Orr[155], V. O'Shea[59], L.M. Osojnak[128], R. Ospanov[62a], G. Otero y Garzon[30], H. Otono[89], P.S. Ott[63a], G.J. Ottino[17a], M. Ouchrif[35d], J. Ouellette[29], F. Ould-Saada[125], M. Owen[59], R.E. Owen[134], K.Y. Oyulmaz[21a], V.E. Ozcan[21a], N. Ozturk[8], S. Ozturk[21d], H.A. Pacey[32], A. Pacheco Pages[13], C. Padilla Aranda[13], G. Padovano[75a,75b], S. Pagan Griso[17a], G. Palacino[68], A. Palazzo[70a,70b], S. Palestini[36], J. Pan[171], T. Pan[64a], D.K. Panchal[11], C.E. Pandini[114], J.G. Panduro Vazquez[95], H. Pang[14b], P. Pani[48], G. Panizzo[69a,69c], L. Paolozzi[56], C. Papadatos[108], S. Parajuli[44], A. Paramonov[6], C. Paraskevopoulos[10], D. Paredes Hernandez[64b], T.H. Park[155], M.A. Parker[32], F. Parodi[57b,57a], E.W. Parrish[115], V.A. Parrish[52], J.A. Parsons[41], U. Parzefall[54], B. Pascual Dias[108], L. Pascual Dominguez[151], F. Pasquali[114], E. Pasqualucci[75a], S. Passaggio[57b], F. Pastore[95], P. Pasuwan[47a,47b], P. Patel[86], U.M. Patel[51], J.R. Pater[101], T. Pauly[36], J. Pearkes[143], M. Pedersen[125], R. Pedro[130a], S.V. Peleganchuk[37], O. Penc[36], E.A. Pender[52], H. Peng[62a], K.E. Penski[109], M. Penzin[37], B.S. Peralva[82d,82d], A.P. Pereira Peixoto[60], L. Pereira Sanchez[47a,47b], D.V. Perepelitsa[29,af], E. Perez Codina[156a], M. Perganti[10], L. Perini[71a,71b,*], H. Pernegger[36], A. Perrevoort[113], O. Perrin[40], K. Peters[48], R.F.Y. Peters[101], B.A. Petersen[36], T.C. Petersen[42], E. Petit[102], V. Petousis[132], C. Petridou[152,e], A. Petrukhin[141], M. Pettee[17a], N.E. Pettersson[36], A. Petukhov[37], K. Petukhova[133], A. Peyaud[135], R. Pezoa[137f], L. Pezzotti[36], G. Pezzullo[171], T.M. Pham[169], T. Pham[105], P.W. Phillips[134], G. Piacquadio[145], E. Pianori[17a], F. Piazza[71a,71b], R. Piegaia[30], D. Pietreanu[27b], A.D. Pilkington[101], M. Pinamonti[69a,69c], J.L. Pinfold[2], B.C. Pinheiro Pereira[130a], A.E. Pinto Pinoargote[135], K.M. Piper[146], C. Pitman Donaldson[96], D.A. Pizzi[34], L. Pizzimento[76a,76b], A. Pizzini[114], M.-A. Pleier[29], V. Plesanovs[54], V. Pleskot[133], E. Plotnikova[38], G. Poddar[4], R. Poettgen[98], L. Poggioli[127], I. Pokharel[55], S. Polacek[133], G. Polesello[73a], A. Poley[142,156a], R. Polifka[132], A. Polini[23b], C.S. Pollard[166], Z.B. Pollock[119], V. Polychronakos[29], E. Pompa Pacchi[75a,75b], D. Ponomarenko[113], L. Pontecorvo[36], S. Popa[27a], G.A. Popeneciu[27d], A. Poreba[36], D.M. Portillo Quintero[156a], S. Pospisil[132], M.A. Postill[139], P. Postolache[27c], K. Potamianos[166],

P.P. Potepa[85a], I.N. Potrap[38], C.J. Potter[32], H. Potti[1], T. Poulsen[48], J. Poveda[162], M.E. Pozo Astigarraga[36], A. Prades Ibanez[162], D. Price[101], M. Primavera[70a], M.A. Principe Martin[99], R. Privara[122], T. Procter[59], M.L. Proffitt[138], N. Proklova[128], K. Prokofiev[64c], G. Proto[76a,76b], S. Protopopescu[29], J. Proudfoot[6], M. Przybycien[85a], W.W. Przygoda[85b], J.E. Puddefoot[139], D. Pudzha[37], D. Pyatiizbyantseva[37], J. Qian[106], D. Qichen[101], Y. Qin[101], T. Qiu[52], A. Quadt[55], M. Queitsch-Maitland[101], G. Quetant[56], G. Rabanal Bolanos[61], D. Rafanoharana[54], F. Ragusa[71a,71b], J.L. Rainbolt[39], J.A. Raine[56], S. Rajagopalan[29], E. Ramakoti[37], K. Ran[48,14e], N.P. Rapheeha[33g], H. Rasheed[27b], V. Raskina[127], D.F. Rassloff[63a], S. Rave[100], B. Ravina[55], I. Ravinovich[168], M. Raymond[36], A.L. Read[125], N.P. Readioff[139], D.M. Rebuzzi[73a,73b], G. Redlinger[29], A.S. Reed[110], K. Reeves[26], J.A. Reidelsturz[170], D. Reikher[151], A. Rej[141], C. Rembser[36], A. Renardi[48], M. Renda[27b], M.B. Rendel[110], F. Renner[48], A.G. Rennie[59], S. Resconi[71a], M. Ressegotti[57b,57a], S. Rettie[36], J.G. Reyes Rivera[107], B. Reynolds[119], E. Reynolds[17a], O.L. Rezanova[37], P. Reznicek[133], N. Ribaric[91], E. Ricci[78a,78b], R. Richter[110], S. Richter[47a,47b], E. Richter-Was[85b], M. Ridel[127], S. Ridouani[35d], P. Rieck[117], P. Riedler[36], M. Rijssenbeek[145], A. Rimoldi[73a,73b], M. Rimoldi[48], L. Rinaldi[23b,23a], T.T. Rinn[29], M.P. Rinnagel[109], G. Ripellino[160], I. Riu[13], P. Rivadeneira[48], J.C. Rivera Vergara[164], F. Rizatdinova[121], E. Rizvi[94], B.A. Roberts[166], B.R. Roberts[17a], S.H. Robertson[104,w], M. Robin[48], D. Robinson[32], C.M. Robles Gajardo[137f], M. Robles Manzano[100], A. Robson[59], A. Rocchi[76a,76b], C. Roda[74a,74b], S. Rodriguez Bosca[63a], Y. Rodriguez Garcia[22a], A. Rodriguez Rodriguez[54], A.M. Rodríguez Vera[156b], S. Roe[36], J.T. Roemer[159], A.R. Roepe-Gier[136], J. Roggel[170], O. Røhne[125], R.A. Rojas[103], C.P.A. Roland[68], J. Roloff[29], A. Romaniouk[37], E. Romano[73a,73b], M. Romano[23b], A.C. Romero Hernandez[161], N. Rompotis[92], L. Roos[127], S. Rosati[75a], B.J. Rosser[39], E. Rossi[126], E. Rossi[72a,72b], L.P. Rossi[57b], L. Rossini[48], R. Rosten[119], M. Rotaru[27b], B. Rottler[54], C. Rougier[102], D. Rousseau[66], D. Rousso[32], A. Roy[161], S. Roy-Garand[155], A. Rozanov[102], Y. Rozen[150], X. Ruan[33g], A. Rubio Jimenez[162], A.J. Ruby[92], V.H. Ruelas Rivera[18], T.A. Ruggeri[1], A. Ruggiero[126], A. Ruiz-Martinez[162], A. Rummler[36], Z. Rurikova[54], N.A. Rusakovich[38], H.L. Russell[164], G. Russo[75a,75b], J.P. Rutherfoord[7], S. Rutherford Colmenares[32], K. Rybacki[91], M. Rybar[133], E.B. Rye[125], A. Ryzhov[44], J.A. Sabater Iglesias[56], P. Sabatini[162], L. Sabetta[75a,75b], H.F-W. Sadrozinski[136], F. Safai Tehrani[75a], B. Safarzadeh Samani[146], M. Safdari[143], S. Saha[164], M. Sahinsoy[110], M. Saimpert[135], M. Saito[153], T. Saito[153], D. Salamani[36], A. Salnikov[143], J. Salt[162], A. Salvador Salas[13], D. Salvatore[43b,43a], F. Salvatore[146], A. Salzburger[36], D. Sammel[54], D. Sampsonidis[152,e], D. Sampsonidou[123], J. Sánchez[162], A. Sanchez Pineda[4], V. Sanchez Sebastian[162], H. Sandaker[125], C.O. Sander[48], J.A. Sandesara[103], M. Sandhoff[170], C. Sandoval[22b], D.P.C. Sankey[134], T. Sano[87], A. Sansoni[53], L. Santi[75a,75b], C. Santoni[40], H. Santos[130a,130b], S.N. Santpur[17a], A. Santra[168], K.A. Saoucha[139], J.G. Saraiva[130a,130d], J. Sardain[7], O. Sasaki[83], K. Sato[157], C. Sauer[63b], F. Sauerburger[54], E. Sauvan[4], P. Savard[155,ad], R. Sawada[153], C. Sawyer[134], L. Sawyer[97], I. Sayago Galvan[162], C. Sbarra[23b], A. Sbrizzi[23b,23a], T. Scanlon[96], J. Schaarschmidt[138], P. Schacht[110], D. Schaefer[39], U. Schäfer[100], A.C. Schaffer[66,44], D. Schaile[109], R.D. Schamberger[145], C. Scharf[18], M.M. Schefer[19], V.A. Schegelsky[37], D. Scheirich[133], F. Schenck[18], M. Schernau[159], C. Scheulen[55], C. Schiavi[57b,57a], E.J. Schioppa[70a,70b], M. Schioppa[43b,43a], B. Schlag[143], K.E. Schleicher[54], S. Schlenker[36], J. Schmeing[170], M.A. Schmidt[170], K. Schmieden[100], C. Schmitt[100], S. Schmitt[48], L. Schoeffel[135], A. Schoening[63b], P.G. Scholer[54], E. Schopf[126], M. Schott[100], J. Schovancova[36], S. Schramm[56], F. Schroeder[170], T. Schroer[56], H-C. Schultz-Coulon[63a], M. Schumacher[54],

B.A. Schumm[136], Ph. Schune[135], A.J. Schuy[138], H.R. Schwartz[136], A. Schwartzman[143], T.A. Schwarz[106], Ph. Schwemling[135], R. Schwienhorst[107], A. Sciandra[136], G. Sciolla[26], F. Scuri[74a], C.D. Sebastiani[92], K. Sedlaczek[115], P. Seema[18], S.C. Seidel[112], A. Seiden[136], B.D. Seidlitz[41], C. Seitz[48], J.M. Seixas[82b], G. Sekhniaidze[72a], S.J. Sekula[44], L. Selem[60], N. Semprini-Cesari[23b,23a], D. Sengupta[56], V. Senthilkumar[162], L. Serin[66], L. Serkin[69a,69b], M. Sessa[76a,76b], H. Severini[120], F. Sforza[57b,57a], A. Sfyrla[56], E. Shabalina[55], R. Shaheen[144], J.D. Shahinian[128], D. Shaked Renous[168], L.Y. Shan[14a], M. Shapiro[17a], A. Sharma[36], A.S. Sharma[163], P. Sharma[80], S. Sharma[48], P.B. Shatalov[37], K. Shaw[146], S.M. Shaw[101], A. Shcherbakova[37], Q. Shen[62c,5], P. Sherwood[96], L. Shi[96], X. Shi[14a], C.O. Shimmin[171], Y. Shimogama[167], J.D. Shinner[95], I.P.J. Shipsey[126], S. Shirabe[56,h], M. Shiyakova[38], J. Shlomi[168], M.J. Shochet[39], J. Shojaii[105], D.R. Shope[125], S. Shrestha[119,ag], E.M. Shrif[33g], M.J. Shroff[164], P. Sicho[131], A.M. Sickles[161], E. Sideras Haddad[33g], A. Sidoti[23b], F. Siegert[50], Dj. Sijacki[15], R. Sikora[85a], F. Sili[90], J.M. Silva[20], M.V. Silva Oliveira[29], S.B. Silverstein[47a], S. Simion[66], R. Simoniello[36], E.L. Simpson[59], H. Simpson[146], L.R. Simpson[106], N.D. Simpson[98], S. Simsek[21d], S. Sindhu[55], P. Sinervo[155], S. Singh[155], S. Sinha[48], S. Sinha[101], M. Sioli[23b,23a], I. Siral[36], E. Sitnikova[48], S.Yu. Sivoklokov[37,*], J. Sjölin[47a,47b], A. Skaf[55], E. Skorda[98], P. Skubic[120], M. Slawinska[86], V. Smakhtin[168], B.H. Smart[134], J. Smiesko[36], S.Yu. Smirnov[37], Y. Smirnov[37], L.N. Smirnova[37,a], O. Smirnova[98], A.C. Smith[41], E.A. Smith[39], H.A. Smith[126], J.L. Smith[92], R. Smith[143], M. Smizanska[91], K. Smolek[132], A.A. Snesarev[37], S.R. Snider[155], H.L. Snoek[114], S. Snyder[29], R. Sobie[164,w], A. Soffer[151], C.A. Solans Sanchez[36], E.Yu. Soldatov[37], U. Soldevila[162], A.A. Solodkov[37], S. Solomon[26], A. Soloshenko[38], K. Solovieva[54], O.V. Solovyanov[40], V. Solovyev[37], P. Sommer[36], A. Sonay[13], W.Y. Song[156b], J.M. Sonneveld[114], A. Sopczak[132], A.L. Sopio[96], F. Sopkova[28b], V. Sothilingam[63a], S. Sottocornola[68], R. Soualah[116c], Z. Soumaimi[35e], D. South[48], S. Spagnolo[70a,70b], M. Spalla[110], D. Sperlich[54], G. Spigo[36], M. Spina[146], S. Spinali[91], D.P. Spiteri[59], M. Spousta[133], E.J. Staats[34], A. Stabile[71a,71b], R. Stamen[63a], M. Stamenkovic[114], A. Stampekis[20], M. Standke[24], E. Stanecka[86], M.V. Stange[50], B. Stanislaus[17a], M.M. Stanitzki[48], B. Stapf[48], E.A. Starchenko[37], G.H. Stark[136], J. Stark[102], D.M. Starko[156b], P. Staroba[131], P. Starovoitov[63a], S. Stärz[104], R. Staszewski[86], G. Stavropoulos[46], J. Steentoft[160], P. Steinberg[29], B. Stelzer[142,156a], H.J. Stelzer[129], O. Stelzer-Chilton[156a], H. Stenzel[58], T.J. Stevenson[146], G.A. Stewart[36], J.R. Stewart[121], M.C. Stockton[36], G. Stoicea[27b], M. Stolarski[130a], S. Stonjek[110], A. Straessner[50], J. Strandberg[144], S. Strandberg[47a,47b], M. Strauss[120], T. Strebler[102], P. Strizenec[28b], R. Ströhmer[165], D.M. Strom[123], L.R. Strom[48], R. Stroynowski[44], A. Strubig[47a,47b], S.A. Stucci[29], B. Stugu[16], J. Stupak[120], N.A. Styles[48], D. Su[143], S. Su[62a], W. Su[62d], X. Su[62a,66], K. Sugizaki[153], V.V. Sulin[37], M.J. Sullivan[92], D.M.S. Sultan[78a,78b], L. Sultanaliyeva[37], S. Sultansoy[3b], T. Sumida[87], S. Sun[106], S. Sun[169], O. Sunneborn Gudnadottir[160], M.R. Sutton[146], H. Suzuki[157], M. Svatos[131], M. Swiatlowski[156a], T. Swirski[165], I. Sykora[28a], M. Sykora[133], T. Sykora[133], D. Ta[100], K. Tackmann[48,u], A. Taffard[159], R. Tafirout[156a], J.S. Tafoya Vargas[66], R. Takashima[88], E.P. Takeva[52], Y. Takubo[83], M. Talby[102], A.A. Talyshev[37], K.C. Tam[64b], N.M. Tamir[151], A. Tanaka[153], J. Tanaka[153], R. Tanaka[66], M. Tanasini[57b,57a], Z. Tao[163], S. Tapia Araya[137f], S. Tapprogge[100], A. Tarek Abouelfadl Mohamed[107], S. Tarem[150], K. Tariq[62b], G. Tarna[102,27b], G.F. Tartarelli[71a], P. Tas[133], M. Tasevsky[131], E. Tassi[43b,43a], A.C. Tate[161], G. Tateno[153], Y. Tayalati[35e,v], G.N. Taylor[105], W. Taylor[156b], H. Teagle[92], A.S. Tee[169], R. Teixeira De Lima[143], P. Teixeira-Dias[95], J.J. Teoh[155], K. Terashi[153], J. Terron[99], S. Terzo[13], M. Testa[53],

R.J. Teuscher[155,w], A. Thaler[79], O. Theiner[56], N. Themistokleous[52], T. Theveneaux-Pelzer[102], O. Thielmann[170], D.W. Thomas[95], J.P. Thomas[20], E.A. Thompson[17a], P.D. Thompson[20], E. Thomson[128], Y. Tian[55], V. Tikhomirov[37,a], Yu.A. Tikhonov[37], S. Timoshenko[37], D. Timoshyn[133], E.X.L. Ting[1], P. Tipton[171], S.H. Tlou[33g], A. Tnourji[40], K. Todome[23b,23a], S. Todorova-Nova[133], S. Todt[50], M. Togawa[83], J. Tojo[89], S. Tokár[28a], K. Tokushuku[83], O. Toldaiev[68], R. Tombs[32], M. Tomoto[83,111], L. Tompkins[143], K.W. Topolnicki[85b], E. Torrence[123], H. Torres[102], E. Torró Pastor[162], M. Toscani[30], C. Tosciri[39], M. Tost[11], D.R. Tovey[139], A. Traeet[16], I.S. Trandafir[27b], T. Trefzger[165], A. Tricoli[29], I.M. Trigger[156a], S. Trincaz-Duvoid[127], D.A. Trischuk[26], B. Trocmé[60], C. Troncon[71a], L. Truong[33c], M. Trzebinski[86], A. Trzupek[86], F. Tsai[145], M. Tsai[106], A. Tsiamis[152,e], P.V. Tsiareshka[37], S. Tsigaridas[156a], A. Tsirigotis[152,s], V. Tsiskaridze[145], E.G. Tskhadadze[149a], M. Tsopoulou[152,e], Y. Tsujikawa[87], I.I. Tsukerman[37], V. Tsulaia[17a], S. Tsuno[83], O. Tsur[150], K. Tsuri[118], D. Tsybychev[145], Y. Tu[64b], A. Tudorache[27b], V. Tudorache[27b], A.N. Tuna[36], S. Turchikhin[38], I. Turk Cakir[3a], R. Turra[71a], T. Turtuvshin[38,x], P.M. Tuts[41], S. Tzamarias[152,e], P. Tzanis[10], E. Tzovara[100], K. Uchida[153], F. Ukegawa[157], P.A. Ulloa Poblete[137c,137b], E.N. Umaka[29], G. Unal[36], M. Unal[11], A. Undrus[29], G. Unel[159], J. Urban[28b], P. Urquijo[105], G. Usai[8], R. Ushioda[154], M. Usman[108], Z. Uysal[21b], L. Vacavant[102], V. Vacek[132], B. Vachon[104], K.O.H. Vadla[125], T. Vafeiadis[36], A. Vaitkus[96], C. Valderanis[109], E. Valdes Santurio[47a,47b], M. Valente[156a], S. Valentinetti[23b,23a], A. Valero[162], E. Valiente Moreno[162], A. Vallier[102], J.A. Valls Ferrer[162], D.R. Van Arneman[114], T.R. Van Daalen[138], A. Van Der Graaf[49], P. Van Gemmeren[6], M. Van Rijnbach[125,36], S. Van Stroud[96], I. Van Vulpen[114], M. Vanadia[76a,76b], W. Vandelli[36], M. Vandenbroucke[135], E.R. Vandewall[121], D. Vannicola[151], L. Vannoli[57b,57a], R. Vari[75a], E.W. Varnes[7], C. Varni[17a], T. Varol[148], D. Varouchas[66], L. Varriale[162], K.E. Varvell[147], M.E. Vasile[27b], L. Vaslin[40], G.A. Vasquez[164], F. Vazeille[40], T. Vazquez Schroeder[36], J. Veatch[31], V. Vecchio[101], M.J. Veen[103], I. Veliscek[126], L.M. Veloce[155], F. Veloso[130a,130c], S. Veneziano[75a], A. Ventura[70a,70b], A. Verbytskyi[110], M. Verducci[74a,74b], C. Vergis[24], M. Verissimo De Araujo[82b], W. Verkerke[114], J.C. Vermeulen[114], C. Vernieri[143], P.J. Verschuuren[95], M. Vessella[103], M.C. Vetterli[142,ad], A. Vgenopoulos[152,e], N. Viaux Maira[137f], T. Vickey[139], O.E. Vickey Boeriu[139], G.H.A. Viehhauser[126], L. Vigani[63b], M. Villa[23b,23a], M. Villaplana Perez[162], E.M. Villhauer[52], E. Vilucchi[53], M.G. Vincter[34], G.S. Virdee[20], A. Vishwakarma[52], A. Visibile[114], C. Vittori[36], I. Vivarelli[146], V. Vladimirov[166], E. Voevodina[110], F. Vogel[109], P. Vokac[132], J. Von Ahnen[48], E. Von Toerne[24], B. Vormwald[36], V. Vorobel[133], K. Vorobev[37], M. Vos[162], K. Voss[141], J.H. Vossebeld[92], M. Vozak[114], L. Vozdecky[94], N. Vranjes[15], M. Vranjes Milosavljevic[15], M. Vreeswijk[114], N.K. Vu[62d,62c], R. Vuillermet[36], O. Vujinovic[100], I. Vukotic[39], S. Wada[157], C. Wagner[103], J.M. Wagner[17a], W. Wagner[170], S. Wahdan[170], H. Wahlberg[90], R. Wakasa[157], M. Wakida[111], J. Walder[134], R. Walker[109], W. Walkowiak[141], A. Wall[128], T. Wamorkar[6], A.Z. Wang[169], C. Wang[100], C. Wang[62c], H. Wang[17a], J. Wang[64a], R.-J. Wang[100], R. Wang[61], R. Wang[6], S.M. Wang[148], S. Wang[62b], T. Wang[62a], W.T. Wang[80], X. Wang[14c], X. Wang[161], X. Wang[62c], Y. Wang[62d], Y. Wang[14c], Z. Wang[106], Z. Wang[62d,51,62c], Z. Wang[106], A. Warburton[104], R.J. Ward[20], N. Warrack[59], A.T. Watson[20], H. Watson[59], M.F. Watson[20], E. Watton[59,134], G. Watts[138], B.M. Waugh[96], C. Weber[29], H.A. Weber[18], M.S. Weber[19], S.M. Weber[63a], C. Wei[62a], Y. Wei[126], A.R. Weidberg[126], E.J. Weik[117], J. Weingarten[49], M. Weirich[100], C. Weiser[54], C.J. Wells[48], T. Wenaus[29], B. Wendland[49], T. Wengler[36], N.S. Wenke[110], N. Wermes[24], M. Wessels[63a], K. Whalen[123], A.M. Wharton[91], A.S. White[61], A. White[8], M.J. White[1], D. Whiteson[159], L. Wickremasinghe[124], W. Wiedenmann[169], C. Wiel[50], M. Wielers[134], C. Wiglesworth[42],

D.J. Wilbern[120], H.G. Wilkens[36], D.M. Williams[41], H.H. Williams[128], S. Williams[32], S. Willocq[103], B.J. Wilson[101], P.J. Windischhofer[39], F.I. Winkel[30], F. Winklmeier[123], B.T. Winter[54], J.K. Winter[101], M. Wittgen[143], M. Wobisch[97], Z. Wolffs[114], R. Wölker[126], J. Wollrath[159], M.W. Wolter[86], H. Wolters[130a,130c], A.F. Wongel[48], S.D. Worm[48], B.K. Wosiek[86], K.W. Woźniak[86], S. Wozniewski[55], K. Wraight[59], C. Wu[20], J. Wu[14a,14e], M. Wu[64a], M. Wu[113], S.L. Wu[169], X. Wu[56], Y. Wu[62a], Z. Wu[135], J. Wuerzinger[110], T.R. Wyatt[101], B.M. Wynne[52], S. Xella[42], L. Xia[14c], M. Xia[14b], J. Xiang[64c], X. Xiao[106], M. Xie[62a], X. Xie[62a], S. Xin[14a,14e], J. Xiong[17a], D. Xu[14a], H. Xu[62a], L. Xu[62a], R. Xu[128], T. Xu[106], Y. Xu[14b], Z. Xu[52], Z. Xu[14a], B. Yabsley[147], S. Yacoob[33a], N. Yamaguchi[89], Y. Yamaguchi[154], E. Yamashita[153], H. Yamauchi[157], T. Yamazaki[17a], Y. Yamazaki[84], J. Yan[62c], S. Yan[126], Z. Yan[25], H.J. Yang[62c,62d], H.T. Yang[62a], S. Yang[62a], T. Yang[64c], X. Yang[62a], X. Yang[14a], Y. Yang[44], Z. Yang[62a], W-M. Yao[17a], Y.C. Yap[48], H. Ye[14c], H. Ye[55], J. Ye[44], S. Ye[29], X. Ye[62a], Y. Yeh[96], I. Yeletskikh[38], B.K. Yeo[17a], M.R. Yexley[96], P. Yin[41], K. Yorita[167], S. Younas[27b], C.J.S. Young[54], C. Young[143], Y. Yu[62a], M. Yuan[106], R. Yuan[62b,k], L. Yue[96], M. Zaazoua[62a], B. Zabinski[86], E. Zaid[52], T. Zakareishvili[149b], N. Zakharchuk[34], S. Zambito[56], J.A. Zamora Saa[137d,137b], J. Zang[153], D. Zanzi[54], O. Zaplatilek[132], C. Zeitnitz[170], H. Zeng[14a], J.C. Zeng[161], D.T. Zenger Jr[26], O. Zenin[37], T. Ženiš[28a], S. Zenz[94], S. Zerradi[35a], D. Zerwas[66], M. Zhai[14a,14e], B. Zhang[14c], D.F. Zhang[139], J. Zhang[62b], J. Zhang[6], K. Zhang[14a,14e], L. Zhang[14c], P. Zhang[14a,14e], R. Zhang[169], S. Zhang[106], T. Zhang[153], X. Zhang[62c], X. Zhang[62b], Y. Zhang[62c,5], Y. Zhang[96], Z. Zhang[17a], Z. Zhang[66], H. Zhao[138], P. Zhao[51], T. Zhao[62b], Y. Zhao[136], Z. Zhao[62a], A. Zhemchugov[38], K. Zheng[161], X. Zheng[62a], Z. Zheng[143], D. Zhong[161], B. Zhou[106], H. Zhou[7], N. Zhou[62c], Y. Zhou[7], C.G. Zhu[62b], J. Zhu[106], Y. Zhu[62c], Y. Zhu[62a], X. Zhuang[14a], K. Zhukov[37], V. Zhulanov[37], N.I. Zimine[38], J. Zinsser[63b], M. Ziolkowski[141], L. Živković[15], A. Zoccoli[23b,23a], K. Zoch[56], T.G. Zorbas[139], O. Zormpa[46], W. Zou[41], L. Zwalinski[36].

[1]Department of Physics, University of Adelaide, Adelaide; Australia.
[2]Department of Physics, University of Alberta, Edmonton AB; Canada.
[3(a)]Department of Physics, Ankara University, Ankara;[(b)]Division of Physics, TOBB University of Economics and Technology, Ankara; Türkiye.
[4]LAPP, Univ. Savoie Mont Blanc, CNRS/IN2P3, Annecy; France.
[5]APC, Université Paris Cité, CNRS/IN2P3, Paris; France.
[6]High Energy Physics Division, Argonne National Laboratory, Argonne IL; United States of America.
[7]Department of Physics, University of Arizona, Tucson AZ; United States of America.
[8]Department of Physics, University of Texas at Arlington, Arlington TX; United States of America.
[9]Physics Department, National and Kapodistrian University of Athens, Athens; Greece.
[10]Physics Department, National Technical University of Athens, Zografou; Greece.
[11]Department of Physics, University of Texas at Austin, Austin TX; United States of America.
[12]Institute of Physics, Azerbaijan Academy of Sciences, Baku; Azerbaijan.
[13]Institut de Física d'Altes Energies (IFAE), Barcelona Institute of Science and Technology, Barcelona; Spain.
[14(a)]Institute of High Energy Physics, Chinese Academy of Sciences, Beijing;[(b)]Physics Department, Tsinghua University, Beijing;[(c)]Department of Physics, Nanjing University, Nanjing;[(d)]School of Science, Shenzhen Campus of Sun Yat-sen University;[(e)]University of Chinese Academy of Science (UCAS), Beijing; China.
[15]Institute of Physics, University of Belgrade, Belgrade; Serbia.

[16]Department for Physics and Technology, University of Bergen, Bergen; Norway.
[17](a)Physics Division, Lawrence Berkeley National Laboratory, Berkeley CA;(b)University of California, Berkeley CA; United States of America.
[18]Institut für Physik, Humboldt Universität zu Berlin, Berlin; Germany.
[19]Albert Einstein Center for Fundamental Physics and Laboratory for High Energy Physics, University of Bern, Bern; Switzerland.
[20]School of Physics and Astronomy, University of Birmingham, Birmingham; United Kingdom.
[21](a)Department of Physics, Bogazici University, Istanbul;(b)Department of Physics Engineering, Gaziantep University, Gaziantep;(c)Department of Physics, Istanbul University, Istanbul;(d)Istinye University, Sariyer, Istanbul; Türkiye.
[22](a)Facultad de Ciencias y Centro de Investigaciónes, Universidad Antonio Nariño, Bogotá;(b)Departamento de Física, Universidad Nacional de Colombia, Bogotá;(c)Pontificia Universidad Javeriana, Bogota; Colombia.
[23](a)Dipartimento di Fisica e Astronomia A. Righi, Università di Bologna, Bologna;(b)INFN Sezione di Bologna; Italy.
[24]Physikalisches Institut, Universität Bonn, Bonn; Germany.
[25]Department of Physics, Boston University, Boston MA; United States of America.
[26]Department of Physics, Brandeis University, Waltham MA; United States of America.
[27](a)Transilvania University of Brasov, Brasov;(b)Horia Hulubei National Institute of Physics and Nuclear Engineering, Bucharest;(c)Department of Physics, Alexandru Ioan Cuza University of Iasi, Iasi;(d)National Institute for Research and Development of Isotopic and Molecular Technologies, Physics Department, Cluj-Napoca;(e)University Politehnica Bucharest, Bucharest;(f)West University in Timisoara, Timisoara;(g)Faculty of Physics, University of Bucharest, Bucharest; Romania.
[28](a)Faculty of Mathematics, Physics and Informatics, Comenius University, Bratislava;(b)Department of Subnuclear Physics, Institute of Experimental Physics of the Slovak Academy of Sciences, Kosice; Slovak Republic.
[29]Physics Department, Brookhaven National Laboratory, Upton NY; United States of America.
[30]Universidad de Buenos Aires, Facultad de Ciencias Exactas y Naturales, Departamento de Física, y CONICET, Instituto de Física de Buenos Aires (IFIBA), Buenos Aires; Argentina.
[31]California State University, CA; United States of America.
[32]Cavendish Laboratory, University of Cambridge, Cambridge; United Kingdom.
[33](a)Department of Physics, University of Cape Town, Cape Town;(b)iThemba Labs, Western Cape;(c)Department of Mechanical Engineering Science, University of Johannesburg, Johannesburg;(d)National Institute of Physics, University of the Philippines Diliman (Philippines);(e)University of South Africa, Department of Physics, Pretoria;(f)University of Zululand, KwaDlangezwa;(g)School of Physics, University of the Witwatersrand, Johannesburg; South Africa.
[34]Department of Physics, Carleton University, Ottawa ON; Canada.
[35](a)Faculté des Sciences Ain Chock, Réseau Universitaire de Physique des Hautes Energies - Université Hassan II, Casablanca;(b)Faculté des Sciences, Université Ibn-Tofail, Kénitra;(c)Faculté des Sciences Semlalia, Université Cadi Ayyad, LPHEA-Marrakech;(d)LPMR, Faculté des Sciences, Université Mohamed Premier, Oujda;(e)Faculté des sciences, Université Mohammed V, Rabat;(f)Institute of Applied Physics, Mohammed VI Polytechnic University, Ben Guerir; Morocco.
[36]CERN, Geneva; Switzerland.
[37]Affiliated with an institute covered by a cooperation agreement with CERN.
[38]Affiliated with an international laboratory covered by a cooperation agreement with CERN.
[39]Enrico Fermi Institute, University of Chicago, Chicago IL; United States of America.
[40]LPC, Université Clermont Auvergne, CNRS/IN2P3, Clermont-Ferrand; France.

[41]Nevis Laboratory, Columbia University, Irvington NY; United States of America.
[42]Niels Bohr Institute, University of Copenhagen, Copenhagen; Denmark.
[43(a)]Dipartimento di Fisica, Università della Calabria, Rende;[(b)]INFN Gruppo Collegato di Cosenza, Laboratori Nazionali di Frascati; Italy.
[44]Physics Department, Southern Methodist University, Dallas TX; United States of America.
[45]Physics Department, University of Texas at Dallas, Richardson TX; United States of America.
[46]National Centre for Scientific Research "Demokritos", Agia Paraskevi; Greece.
[47(a)]Department of Physics, Stockholm University;[(b)]Oskar Klein Centre, Stockholm; Sweden.
[48]Deutsches Elektronen-Synchrotron DESY, Hamburg and Zeuthen; Germany.
[49]Fakultät Physik , Technische Universität Dortmund, Dortmund; Germany.
[50]Institut für Kern- und Teilchenphysik, Technische Universität Dresden, Dresden; Germany.
[51]Department of Physics, Duke University, Durham NC; United States of America.
[52]SUPA - School of Physics and Astronomy, University of Edinburgh, Edinburgh; United Kingdom.
[53]INFN e Laboratori Nazionali di Frascati, Frascati; Italy.
[54]Physikalisches Institut, Albert-Ludwigs-Universität Freiburg, Freiburg; Germany.
[55]II. Physikalisches Institut, Georg-August-Universität Göttingen, Göttingen; Germany.
[56]Département de Physique Nucléaire et Corpusculaire, Université de Genève, Genève; Switzerland.
[57(a)]Dipartimento di Fisica, Università di Genova, Genova;[(b)]INFN Sezione di Genova; Italy.
[58]II. Physikalisches Institut, Justus-Liebig-Universität Giessen, Giessen; Germany.
[59]SUPA - School of Physics and Astronomy, University of Glasgow, Glasgow; United Kingdom.
[60]LPSC, Université Grenoble Alpes, CNRS/IN2P3, Grenoble INP, Grenoble; France.
[61]Laboratory for Particle Physics and Cosmology, Harvard University, Cambridge MA; United States of America.
[62(a)]Department of Modern Physics and State Key Laboratory of Particle Detection and Electronics, University of Science and Technology of China, Hefei;[(b)]Institute of Frontier and Interdisciplinary Science and Key Laboratory of Particle Physics and Particle Irradiation (MOE), Shandong University, Qingdao;[(c)]School of Physics and Astronomy, Shanghai Jiao Tong University, Key Laboratory for Particle Astrophysics and Cosmology (MOE), SKLPPC, Shanghai;[(d)]Tsung-Dao Lee Institute, Shanghai; China.
[63(a)]Kirchhoff-Institut für Physik, Ruprecht-Karls-Universität Heidelberg, Heidelberg;[(b)]Physikalisches Institut, Ruprecht-Karls-Universität Heidelberg, Heidelberg; Germany.
[64(a)]Department of Physics, Chinese University of Hong Kong, Shatin, N.T., Hong Kong;[(b)]Department of Physics, University of Hong Kong, Hong Kong;[(c)]Department of Physics and Institute for Advanced Study, Hong Kong University of Science and Technology, Clear Water Bay, Kowloon, Hong Kong; China.
[65]Department of Physics, National Tsing Hua University, Hsinchu; Taiwan.
[66]IJCLab, Université Paris-Saclay, CNRS/IN2P3, 91405, Orsay; France.
[67]Centro Nacional de Microelectrónica (IMB-CNM-CSIC), Barcelona; Spain.
[68]Department of Physics, Indiana University, Bloomington IN; United States of America.
[69(a)]INFN Gruppo Collegato di Udine, Sezione di Trieste, Udine;[(b)]ICTP, Trieste;[(c)]Dipartimento Politecnico di Ingegneria e Architettura, Università di Udine, Udine; Italy.
[70(a)]INFN Sezione di Lecce;[(b)]Dipartimento di Matematica e Fisica, Università del Salento, Lecce; Italy.
[71(a)]INFN Sezione di Milano;[(b)]Dipartimento di Fisica, Università di Milano, Milano; Italy.
[72(a)]INFN Sezione di Napoli;[(b)]Dipartimento di Fisica, Università di Napoli, Napoli; Italy.
[73(a)]INFN Sezione di Pavia;[(b)]Dipartimento di Fisica, Università di Pavia, Pavia; Italy.
[74(a)]INFN Sezione di Pisa;[(b)]Dipartimento di Fisica E. Fermi, Università di Pisa, Pisa; Italy.
[75(a)]INFN Sezione di Roma;[(b)]Dipartimento di Fisica, Sapienza Università di Roma, Roma; Italy.
[76(a)]INFN Sezione di Roma Tor Vergata;[(b)]Dipartimento di Fisica, Università di Roma Tor Vergata, Roma; Italy.

[77](a) INFN Sezione di Roma Tre;(b) Dipartimento di Matematica e Fisica, Università Roma Tre, Roma; Italy.
[78](a) INFN-TIFPA;(b) Università degli Studi di Trento, Trento; Italy.
[79] Universität Innsbruck, Department of Astro and Particle Physics, Innsbruck; Austria.
[80] University of Iowa, Iowa City IA; United States of America.
[81] Department of Physics and Astronomy, Iowa State University, Ames IA; United States of America.
[82](a) Departamento de Engenharia Elétrica, Universidade Federal de Juiz de Fora (UFJF), Juiz de Fora;(b) Universidade Federal do Rio De Janeiro COPPE/EE/IF, Rio de Janeiro;(c) Instituto de Física, Universidade de São Paulo, São Paulo;(d) Rio de Janeiro State University, Rio de Janeiro; Brazil.
[83] KEK, High Energy Accelerator Research Organization, Tsukuba; Japan.
[84] Graduate School of Science, Kobe University, Kobe; Japan.
[85](a) AGH University of Science and Technology, Faculty of Physics and Applied Computer Science, Krakow;(b) Marian Smoluchowski Institute of Physics, Jagiellonian University, Krakow; Poland.
[86] Institute of Nuclear Physics Polish Academy of Sciences, Krakow; Poland.
[87] Faculty of Science, Kyoto University, Kyoto; Japan.
[88] Kyoto University of Education, Kyoto; Japan.
[89] Research Center for Advanced Particle Physics and Department of Physics, Kyushu University, Fukuoka ; Japan.
[90] Instituto de Física La Plata, Universidad Nacional de La Plata and CONICET, La Plata; Argentina.
[91] Physics Department, Lancaster University, Lancaster; United Kingdom.
[92] Oliver Lodge Laboratory, University of Liverpool, Liverpool; United Kingdom.
[93] Department of Experimental Particle Physics, Jožef Stefan Institute and Department of Physics, University of Ljubljana, Ljubljana; Slovenia.
[94] School of Physics and Astronomy, Queen Mary University of London, London; United Kingdom.
[95] Department of Physics, Royal Holloway University of London, Egham; United Kingdom.
[96] Department of Physics and Astronomy, University College London, London; United Kingdom.
[97] Louisiana Tech University, Ruston LA; United States of America.
[98] Fysiska institutionen, Lunds universitet, Lund; Sweden.
[99] Departamento de Física Teorica C-15 and CIAFF, Universidad Autónoma de Madrid, Madrid; Spain.
[100] Institut für Physik, Universität Mainz, Mainz; Germany.
[101] School of Physics and Astronomy, University of Manchester, Manchester; United Kingdom.
[102] CPPM, Aix-Marseille Université, CNRS/IN2P3, Marseille; France.
[103] Department of Physics, University of Massachusetts, Amherst MA; United States of America.
[104] Department of Physics, McGill University, Montreal QC; Canada.
[105] School of Physics, University of Melbourne, Victoria; Australia.
[106] Department of Physics, University of Michigan, Ann Arbor MI; United States of America.
[107] Department of Physics and Astronomy, Michigan State University, East Lansing MI; United States of America.
[108] Group of Particle Physics, University of Montreal, Montreal QC; Canada.
[109] Fakultät für Physik, Ludwig-Maximilians-Universität München, München; Germany.
[110] Max-Planck-Institut für Physik (Werner-Heisenberg-Institut), München; Germany.
[111] Graduate School of Science and Kobayashi-Maskawa Institute, Nagoya University, Nagoya; Japan.
[112] Department of Physics and Astronomy, University of New Mexico, Albuquerque NM; United States of America.
[113] Institute for Mathematics, Astrophysics and Particle Physics, Radboud University/Nikhef, Nijmegen; Netherlands.
[114] Nikhef National Institute for Subatomic Physics and University of Amsterdam, Amsterdam;

Netherlands.
[115]Department of Physics, Northern Illinois University, DeKalb IL; United States of America.
[116(a)]New York University Abu Dhabi, Abu Dhabi;[(b)]United Arab Emirates University, Al Ain;[(c)]University of Sharjah, Sharjah; United Arab Emirates.
[117]Department of Physics, New York University, New York NY; United States of America.
[118]Ochanomizu University, Otsuka, Bunkyo-ku, Tokyo; Japan.
[119]Ohio State University, Columbus OH; United States of America.
[120]Homer L. Dodge Department of Physics and Astronomy, University of Oklahoma, Norman OK; United States of America.
[121]Department of Physics, Oklahoma State University, Stillwater OK; United States of America.
[122]Palacký University, Joint Laboratory of Optics, Olomouc; Czech Republic.
[123]Institute for Fundamental Science, University of Oregon, Eugene, OR; United States of America.
[124]Graduate School of Science, Osaka University, Osaka; Japan.
[125]Department of Physics, University of Oslo, Oslo; Norway.
[126]Department of Physics, Oxford University, Oxford; United Kingdom.
[127]LPNHE, Sorbonne Université, Université Paris Cité, CNRS/IN2P3, Paris; France.
[128]Department of Physics, University of Pennsylvania, Philadelphia PA; United States of America.
[129]Department of Physics and Astronomy, University of Pittsburgh, Pittsburgh PA; United States of America.
[130(a)]Laboratório de Instrumentação e Física Experimental de Partículas - LIP, Lisboa;[(b)]Departamento de Física, Faculdade de Ciências, Universidade de Lisboa, Lisboa;[(c)]Departamento de Física, Universidade de Coimbra, Coimbra;[(d)]Centro de Física Nuclear da Universidade de Lisboa, Lisboa;[(e)]Departamento de Física, Universidade do Minho, Braga;[(f)]Departamento de Física Teórica y del Cosmos, Universidad de Granada, Granada (Spain);[(g)]Instituto Superior Técnico, Universidade de Lisboa, Lisboa; Portugal.
[131]Institute of Physics of the Czech Academy of Sciences, Prague; Czech Republic.
[132]Czech Technical University in Prague, Prague; Czech Republic.
[133]Charles University, Faculty of Mathematics and Physics, Prague; Czech Republic.
[134]Particle Physics Department, Rutherford Appleton Laboratory, Didcot; United Kingdom.
[135]IRFU, CEA, Université Paris-Saclay, Gif-sur-Yvette; France.
[136]Santa Cruz Institute for Particle Physics, University of California Santa Cruz, Santa Cruz CA; United States of America.
[137(a)]Departamento de Física, Pontificia Universidad Católica de Chile, Santiago;[(b)]Millennium Institute for Subatomic physics at high energy frontier (SAPHIR), Santiago;[(c)]Instituto de Investigación Multidisciplinario en Ciencia y Tecnología, y Departamento de Física, Universidad de La Serena;[(d)]Universidad Andres Bello, Department of Physics, Santiago;[(e)]Instituto de Alta Investigación, Universidad de Tarapacá, Arica;[(f)]Departamento de Física, Universidad Técnica Federico Santa María, Valparaíso; Chile.
[138]Department of Physics, University of Washington, Seattle WA; United States of America.
[139]Department of Physics and Astronomy, University of Sheffield, Sheffield; United Kingdom.
[140]Department of Physics, Shinshu University, Nagano; Japan.
[141]Department Physik, Universität Siegen, Siegen; Germany.
[142]Department of Physics, Simon Fraser University, Burnaby BC; Canada.
[143]SLAC National Accelerator Laboratory, Stanford CA; United States of America.
[144]Department of Physics, Royal Institute of Technology, Stockholm; Sweden.
[145]Departments of Physics and Astronomy, Stony Brook University, Stony Brook NY; United States of America.
[146]Department of Physics and Astronomy, University of Sussex, Brighton; United Kingdom.

[147]School of Physics, University of Sydney, Sydney; Australia.
[148]Institute of Physics, Academia Sinica, Taipei; Taiwan.
[149(a)]E. Andronikashvili Institute of Physics, Iv. Javakhishvili Tbilisi State University, Tbilisi;[(b)]High Energy Physics Institute, Tbilisi State University, Tbilisi;[(c)]University of Georgia, Tbilisi; Georgia.
[150]Department of Physics, Technion, Israel Institute of Technology, Haifa; Israel.
[151]Raymond and Beverly Sackler School of Physics and Astronomy, Tel Aviv University, Tel Aviv; Israel.
[152]Department of Physics, Aristotle University of Thessaloniki, Thessaloniki; Greece.
[153]International Center for Elementary Particle Physics and Department of Physics, University of Tokyo, Tokyo; Japan.
[154]Department of Physics, Tokyo Institute of Technology, Tokyo; Japan.
[155]Department of Physics, University of Toronto, Toronto ON; Canada.
[156(a)]TRIUMF, Vancouver BC;[(b)]Department of Physics and Astronomy, York University, Toronto ON; Canada.
[157]Division of Physics and Tomonaga Center for the History of the Universe, Faculty of Pure and Applied Sciences, University of Tsukuba, Tsukuba; Japan.
[158]Department of Physics and Astronomy, Tufts University, Medford MA; United States of America.
[159]Department of Physics and Astronomy, University of California Irvine, Irvine CA; United States of America.
[160]Department of Physics and Astronomy, University of Uppsala, Uppsala; Sweden.
[161]Department of Physics, University of Illinois, Urbana IL; United States of America.
[162]Instituto de Física Corpuscular (IFIC), Centro Mixto Universidad de Valencia - CSIC, Valencia; Spain.
[163]Department of Physics, University of British Columbia, Vancouver BC; Canada.
[164]Department of Physics and Astronomy, University of Victoria, Victoria BC; Canada.
[165]Fakultät für Physik und Astronomie, Julius-Maximilians-Universität Würzburg, Würzburg; Germany.
[166]Department of Physics, University of Warwick, Coventry; United Kingdom.
[167]Waseda University, Tokyo; Japan.
[168]Department of Particle Physics and Astrophysics, Weizmann Institute of Science, Rehovot; Israel.
[169]Department of Physics, University of Wisconsin, Madison WI; United States of America.
[170]Fakultät für Mathematik und Naturwissenschaften, Fachgruppe Physik, Bergische Universität Wuppertal, Wuppertal; Germany.
[171]Department of Physics, Yale University, New Haven CT; United States of America.
[a] Also Affiliated with an institute covered by a cooperation agreement with CERN.
[b] Also at APC, Université Paris Cité, CNRS/IN2P3, Paris; France.
[c] Also at Borough of Manhattan Community College, City University of New York, New York NY; United States of America.
[d] Also at Center for High Energy Physics, Peking University; China.
[e] Also at Center for Interdisciplinary Research and Innovation (CIRI-AUTH), Thessaloniki ; Greece.
[f] Also at Centro Studi e Ricerche Enrico Fermi; Italy.
[g] Also at CERN, Geneva; Switzerland.
[h] Also at Département de Physique Nucléaire et Corpusculaire, Université de Genève, Genève; Switzerland.
[i] Also at Departament de Fisica de la Universitat Autonoma de Barcelona, Barcelona; Spain.
[j] Also at Department of Financial and Management Engineering, University of the Aegean, Chios; Greece.
[k] Also at Department of Physics and Astronomy, Michigan State University, East Lansing MI; United States of America.
[l] Also at Department of Physics and Astronomy, University of Victoria, Victoria BC; Canada.
[m] Also at Department of Physics, California State University, Sacramento; United States of America.

[n] Also at Department of Physics, King's College London, London; United Kingdom.
[o] Also at Department of Physics, Royal Holloway University of London, Egham; United Kingdom.
[p] Also at Department of Physics, University of Fribourg, Fribourg; Switzerland.
[q] Also at Department of Physics, University of Thessaly; Greece.
[r] Also at Department of Physics, Westmont College, Santa Barbara; United States of America.
[s] Also at Hellenic Open University, Patras; Greece.
[t] Also at Institucio Catalana de Recerca i Estudis Avancats, ICREA, Barcelona; Spain.
[u] Also at Institut für Experimentalphysik, Universität Hamburg, Hamburg; Germany.
[v] Also at Institute of Applied Physics, Mohammed VI Polytechnic University, Ben Guerir; Morocco.
[w] Also at Institute of Particle Physics (IPP); Canada.
[x] Also at Institute of Physics and Technology, Ulaanbaatar; Mongolia.
[y] Also at Institute of Physics, Azerbaijan Academy of Sciences, Baku; Azerbaijan.
[z] Also at Institute of Theoretical Physics, Ilia State University, Tbilisi; Georgia.
[aa] Also at KEK, High Energy Accelerator Research Organization, Tsukuba; Japan.
[ab] Also at Lawrence Livermore National Laboratory, Livermore; United States of America.
[ac] Also at The Collaborative Innovation Center of Quantum Matter (CICQM), Beijing; China.
[ad] Also at TRIUMF, Vancouver BC; Canada.
[ae] Also at Università di Napoli Parthenope, Napoli; Italy.
[af] Also at University of Colorado Boulder, Department of Physics, Colorado; United States of America.
[ag] Also at Washington College, Chestertown, MD; United States of America.
[*] Deceased